Tellus
SERIES B
CHEMICAL
AND PHYSICAL
METEOROLOGY
PUBLISHED BY THE INTERNATIONAL METEOROLOGICAL INSTITUTE IN STOCKHOLM

Tellus (2011), 63B, 266–286
Printed in Singapore. All rights reserved

TELLUS

Interannual variability in estimated biological productivity in the Australian sector of the Southern Ocean in 1997–2007

By BARBARA M. JOHNSTON* and ALBERT J. GABRIC, *Australian Rivers Institute, Griffith University, Nathan, QLD 4111, Australia*

(Manuscript received 6 July 2010; in final form 27 December 2010)

ABSTRACT

Changes in biological productivity in the Southern Ocean have the potential to have a significant effect on world climate. Here we use a combination of satellite, model and model reanalysis data to examine climate variability in the Australian sector of the Southern Ocean (110–160°E, 40–70°S) to identify the controls on chlorophyll-*a* (a proxy for phytoplankton biomass) and primary productivity and evaluate trends in these controls over the period 1997–2007.

In summer, in the 65–70°S zone, sea-ice concentration together with the Southern Annular Mode explains 51% of the variance in chlorophyll-*a*, while mean wind stress and sea-surface temperature explains 55% of the variance in the 60–65°S zone. Further north, key controls are photosynthetically active radiation, sea-surface temperature, mixed layer depth and stratification.

Trends in hydrodynamic variables are found to often be opposite in sign and up to an order of magnitude larger than those previously identified in the same sector for 1958–2005. Allowing for the effect of shorter time series on the magnitude of the trends, many recent trends seem to be outside the range of previous variability. These results are consistent with a shift in the ocean state in the past 10–15 yr, in response to a shift in climate.

1. Introduction

Despite the Southern Ocean being characterized as a 'high-nutrient low chlorophyll' region (Whitehouse et al., 2008), physical and concomitant biological changes in the Southern Ocean may exert a disproportionate effect on the world's climate. This is due partly to the circumpolar nature of the Antarctic Circumpolar Current (ACC), which facilitates the movement of heat and CO_2 between the Indian, Pacific and Atlantic Oceans. In addition, Southern Hemisphere westerlies, which drive the ACC, cause divergence-driven upwelling of Upper Circumpolar Deep Water (UCDW), which is rich in CO_2 and nutrients (in particular iron), with potential impacts on both the regional solubility and biological pumps. A study by Lovenduski and Gruber (2005) found that enhanced westerly winds over the Antarctic Zone and Polar Frontal Zone, associated with positive phases of the Southern Annular Mode (SAM), drive increased northward Ekman transport of this nutrient-enriched water, which can affect biology as far north as the Polar Front (Hoppema et al., 2003). A later modelling study by Lovenduski et al. (2007) found that positive phases of the SAM are also associated with anomalous outgassing of natural CO_2, which is only slightly mitigated by the increased uptake of anthropogenic CO_2, leading to a reduction in the rate of increase of CO_2 uptake in the Southern Ocean in the last 50 yr. Other studies, using repeated surface-ocean CO_2 observations (Metzl, 2009; Takahashi et al., 2009) or an inverse method combined with observed atmospheric CO_2 concentrations (Le Quere et al., 2007) have also found that the Southern Ocean carbon sink has been weakening since at least 1990.

To some extent it is possible to assess mid- to late-twentieth century trends for hydrodynamic variables in the Southern Ocean via observations in specific areas at different times (Gille, 2002, 2008; Aoki et al., 2003; Hill et al., 2008) or via climatologies (Boyer et al., 2005; Levitus et al., 2005; Jacobs, 2006; Böning et al., 2008). Other methods include the use of reanalysis data sets, such as the Simple Ocean Data Assimilation (SODA) data set (Yang et al., 2007; Johnston and Gabric, 2010) or modelling studies (Trenberth et al., 2007; Zhang, 2007; Henson et al., 2010).

However, such trends are more difficult to establish for primary productivity, due to the sparse nature of the observational data. The advent of the satellite era, and, in particular the Sea-viewing Wide Field of View Sensor (SeaWiFS, McClain et al.,

*Corresponding author.
e-mail: Barbara.Johnston@griffith.edu.au.
DOI: 10.1111/j.1600-0889.2011.00526.x

2004), has provided an opportunity to consider trends in standing stock (surface chlorophyll-*a*) or primary productivity since 1997. There are, however, caveats associated with reporting trends in satellite-derived chlorophyll-*a* and in using ocean colour models to estimate primary productivity (Saba et al., 2010a,b). One is associated with potential over- or underestimation of the magnitude and variability of primary productivity and the other relates to estimating trends in primary productivity. For example, a recent paper by Saba et al. (2010b) found that, in two Northern Hemisphere subtropical gyres, ocean colour models were more challenged at estimating productivity trends over short time periods (such as the SeaWiFS era) than longer time periods.

A few modelling studies, which use satellite-derived surface chlorophyll-*a* values to calculate primary productivity, have examined trends for the Southern Ocean (Barbini et al., 2005; Arrigo et al., 2008; Smith and Comiso, 2008). Using an algorithm calibrated specifically for use in the Southern Ocean, Arrigo et al. (2008) found no trend in 1997–2006 for annual primary productivity in the whole Southern Ocean, although statistically significant trends for primary productivity in the Ross Sea (increasing) and the south Indian Ocean sector (decreasing) were found. In contrast, Smith and Comiso (2008) found annual productivity over the entire Southern Ocean, calculated using the Vertically Generated Production Algorithm (VGPM) of Behrenfeld and Falkowski (1997), has increased significantly since 1998, particularly in January and February. A recent modelling study (Steinacher et al., 2010), which looks at primary productivity projected over the 21st century, found that, for parts of the Southern Ocean, an alleviation of the limitations of light and/or temperature will lead to an increase in primary productivity, but that absolute change in productivity in the Southern Ocean (south of 45°S) will vary regionally. The variation in trends, in both surface chlorophyll-*a* and primary productivity, between different regions of the Southern Ocean is also illustrated in the work of Martinez et al. (2009), who examine changes in surface chlorophyll-*a* from (1979–1983) to (1998–2002), using data from the earlier Coastal Zone Colour Scanner (CZCS) and SeaWiFS.

Previous work (Steinacher et al., 2010) has identified a number of physiochemical controls on primary productivity in the Southern Ocean. These include sea-ice concentration/extent (near the Antarctic continent), sea-surface temperature (SST), photosynthetically active radiation (PAR), mixed layer depth (MLD), stratification, macro- and micronutrient availability and community composition and grazing. Sea-ice retreat south of 60°S during spring and summer is thought to affect primary productivity by seeding the upper ocean with phytoplankton cells growing in or on the ice, providing a source of iron in meltwater (Constable et al., 2003) and by forming a low salinity, stable surface layer (Smith and Nelson, 1985).

Studies have shown that there is an inverse correlation between MLD and primary productivity (Mitchell and Holm-Hansen, 1991) and the depth of the chlorophyll-*a* maximum (de Baar et al., 2005). Increased wind stress may lead to increased entrainment of nutrients into the mixed layer, but this may be offset by a deepening of the mixed layer, which results in a reduced average light exposure for algal cells. Increased stratification due to increased temperature may also be counterbalanced by increased wind stress. Smith and Comiso (2008) suggest that for open ocean waters, phytoplankton biomass is limited over large regions of the Southern Ocean, due to the interactive effects of iron and irradiance. The availability of key nutrients such as iron and silicic acid (Moore and Doney, 2006) is thought to be related to the strength and upwelling position of nutrient-rich UCDW, which may affect primary productivity and cause shifts of ecosystem structure (Nicol et al., 2000). In addition, a combination of increased temperature and increased iron has been shown to have a magnified effect on primary productivity, compared with the effect of either individually (Rose et al., 2009).

Climate variability can affect many of these controls on primary productivity, particularly on interannual timescales (Boyce et al., 2010). This has been established by considering correlations between chlorophyll-*a* or primary productivity and climate indices, such as the SAM (Marshall, 2003), the Multivariate El Niño/Southern Oscillation (ENSO) Index (Wolter and Timlin, 1993, MEI) and the Pacific Decadal Oscillation (PDO, Mantua and Hare, 2002). For example, studies have shown the link between the SAM and chlorophyll-*a* (Lovenduski and Gruber, 2005), the SAM and primary production (Arrigo et al., 2008), the MEI and chlorophyll-*a* (Behrenfeld et al., 2006) and the PDO index and chlorophyll-*a* (Martinez et al., 2009).

The first aim of this work is to examine how climate variability on interannual timescales affects phytoplankton biomass and primary productivity in the Australian sector of the Southern Ocean, from the Subantarctic zone to the Antarctic continent. The second aim is to identify any trends in these controls over the study period (September 1997–August 2007) and to attempt to set these trends in the context of a longer time-frame. We utilize three types of data: satellite data (for surface chlorophyll-*a*, PAR and sea-ice concentration), modelled primary productivity data (calculated with the VGPM model of Behrenfeld and Falkowski (1997)) and model reanalysis data (SODA for hydrodynamic variables). Seasonal time series (spring and summer), over the study period, are constructed for 5° latitudinal zones that approximate the Southern Ocean frontal zones. These are then correlated with similar surface chlorophyll-*a* time series, in order to identify controls on phytoplankton biomass. In addition, non-parametric methods are used to identify trends in the various variables and, in the case of the hydrodynamic variables, the trends are compared with trends over the period 1958–2005 previously analysed by Johnston and Gabric (2010). Finally, the trends in various hydrodynamic variables are plotted as 'running' sets of trends, beginning with 1958–2007, then 1959–2007 and finishing with 1998–2007, to see if the present trends are outside the range of earlier variability.

2. Methods

2.1. Study region

The region studied in this work is the Australian sector of the Southern Ocean (110–160°E, 40–70°S). This is shown in Fig. 1, which presents mean (1998–2007) SeaWiFS chlorophyll-*a* and VGPM primary productivity for January. Note: in the remainder of this study the words chlorophyll-*a* and primary productivity will be taken to refer to surface chlorophyll-*a* and estimated primary productivity, respectively, in the interests of brevity. Mean positions for the Polar Front and Southern Boundary of the ACC (Orsi and Ryan 2001 updated, 2006) in the Australian sector are also shown in Fig. 1. Approximate mean positions for the other ACC fronts in this region can be taken from those identified on the WOCE SR3 line (approximately 140°E) (Sokolov and Rintoul, 2002): Subantarctic Fronts 1 and 2 (50.5°S and 52°S) and the Southern ACC front (62–64°S). Along this line, the sea-ice zone extends north to approximately 60°S, with seasonal sea-ice retreat to 65°S (Sokolov, 2008).

2.2. Data sources

2.2.1. Satellite data. Chlorophyll-*a* and PAR are derived from SeaWiFS (Version 5.1) (McClain et al., 2004) level 3 monthly

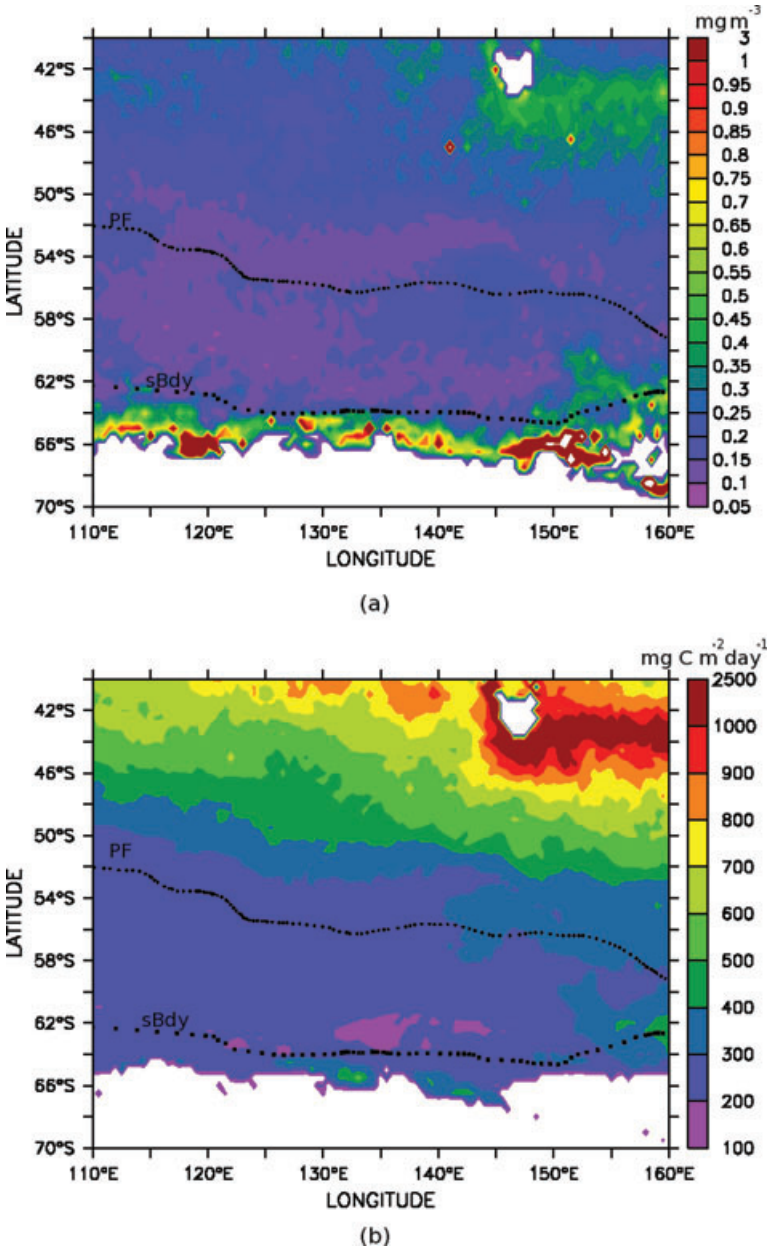

Fig. 1. Mean (1998–2007) January values for (a) SeaWiFS chlorophyll-*a* and (b) VGPM primary productivity, overlaid by the PF and sBdy (Orsi and Ryan 2001 updated, 2006).

data which is gridded at 9 km × 9 km resolution. Monthly sea-ice concentration data (Comiso 1999 updated, 2008) are derived using measurements from the Scanning Multichannel Microwave Radiometer on the Nimbus-7 satellite and the Defense Meteorological Satellite Program Special Sensor Microwave Imagers. Data were generated using the Microwave Scanning Radiometer-Earth Observing System Bootstrap algorithm and gridded on a polar stereographic grid at 25 km × 25 km resolution.

2.2.2. Model data. Net Primary Productivity is computed using the Vertically Generalized Production Model (VGPM) (Behrenfeld and Falkowski, 1997), which estimates primary productivity from chlorophyll-*a* using a temperature-dependent description of chlorophyll-specific photosynthetic efficiency. Our study uses the VGPM output, with the caveat that this is a standard algorithm and is not calibrated specifically for the Southern Ocean. However, the VGPM is a widely used model (Carr et al., 2006) that has been used previously in the Southern Ocean (Behrenfeld et al., 2006; Smith and Comiso, 2008) and most of the other available models are calibrated for specific regions of the Southern Ocean, such as the Ross Sea, but not for the Australian sector (Dierssen et al., 2000; Smith et al., 2000; Barbini et al., 2005). Also, a recent paper Saba et al. (2010a), comparing ocean colour model estimates of primary productivity in the Southern Ocean, found that the VGPM estimated primary productivity well compared with other models. However, it is also worth noting that the authors also found that most ocean colour models overestimated primary productivity but underestimated its variability in the Southern Ocean, which may mean that this work may also under-estimate variability in primary productivity.

SeaWiFS chlorophyll-*a* and PAR data, as well as SST data from the Advanced Very High Resolution Radiometer (AVHRR) are inputs to the VGPM (Behrenfeld and Falkowski, 1997) model, where primary productivity (PP) is defined as

$$\mathrm{PP} = 0.66125 * P^{B}_{\mathrm{opt}} * \frac{E_0}{(E_0 + 4.1)} * chla * Z_{eu} * D_{\mathrm{irr}} \qquad (1)$$

and primary productivity is in units of mg C m^{-2} d^{-1}, P^{B}_{opt} is the optimal rate of photosynthesis in the water column [mg C (mg chlorophyll-*a*)$^{-1}$ h^{-1}] and is regulated by temperature, E_0 is the daily surface PAR (Einsteins m^{-2} d^{-1}), *chla* is chlorophyll-*a* concentration (mg m^{-3}), Z_{eu} is the depth of the euphotic zone (m) and D_{irr} is the photo period (h). Physiological variability is linked to the P^{B}_{opt} variable, which is given by fitting a polynomial of the form, $P^{B}_{\mathrm{opt}} = \sum_{i=0}^{7} a_i (\frac{SST}{10})^i$, to field data (see Behrenfeld and Falkowski, 1997, for the a_i values). The euphotic depth Z_{eu} is calculated from *chla* using the Case I model of Morel and Berthon (1989). Primary productivity is calculated on a daily basis, then binned to give 8-d or monthly values. Monthly primary productivity data sets on a 9 km × 9 km grid are used in this study.

2.2.3. The SODA reanalysis. The Simple Ocean Data Assimilation (SODA) data (Carton et al., 2000; Carton and Giese, 2008) come from a reanalysis of ocean climate variability that begins with a state forecast produced by the Parallel Ocean Program (POP) general circulation model (at 0.25° × 0.4° × 40 level resolution). SODA then uses a sequential data estimation scheme to change temperature and salinity in the model ocean in order to accommodate hydrographic observations, which are restricted to depths shallower than about 1000 m for assimilation, due to the scarcity of observations below that depth. Freshwater fluxes since 1979 come from the Global Precipitation Climatology Project precipitation data and evaporation from bulk formulae (Schott et al., 2009). The vertical diffusion of momentum, heat and salt are carried out using KPP (Large et al., 1994) mixing with modifications to address issues such as diurnal heating (Carton and Giese, 2008). The reanalysis has been evaluated by comparisons with independent observations, such as the historical archive of hydrographic profiles, supplemented by ship intake measurements, moored hydrographic observations, remotely sensed SST and sea level. Comparisons of forecasts and observations, using tide gauge level records and satellite altimetry, are also carried out (Carton et al., 2000).

The remainder of the variables used in this study come either from the SODA reanalysis data set or are derived from variables therein. This work uses the SODA 2.0.2/2.0.4 (1958–2001/2002–2007) data sets to look at the 10 yr period September 1997 to August 2007. The data sets include sea surface heights, surface wind stress, zonal, meridional and vertical velocity fields, as well as temperature and salinity, and are presented on a 0.5° × 0.5° × 40 depth level (from 5 m to about 5500 m, with 10 m resolution in the top 100 m) global grid. The SODA 2.0.4 reanalysis is different from the one for the earlier period in that it uses QuikSCAT (Spencer et al., 2000) winds rather than ERA-40 (Uppala et al., 2005) winds. This is a potential source of error in this work, although the two have been used together in other studies, for example (Schott et al., 2008, 2009; Zheng and Giese, 2009), and examination of the aggregated time series used here does not show any particular biases. While the majority of this work uses the SODA monthly data sets, we have also used the SODA 5-d data, to allow for more accurate detection of UCDW in the mixed layer.

The core of UCDW can be identified (Sievers and Nowlin, 1984; Orsi et al., 1995) by [O_2] < 201 μmol l^{-1} at density values $27.35 < \sigma_\theta < 27.75$ kg m^{-3}, where [O_2] is oxygen concentration and σ_θ is potential density anomaly. This is is equivalent to the density criterion with temperature, $\theta > 1.5$ °C (Orsi et al., 1995; Sokolov and Rintoul, 2002) and gives a salinity range of between 34.5 and 34.7. UCDW is identified in SODA using the density and temperature criteria above.

In order to assess SODA's ability to represent hydrodynamic data in the Southern Ocean, a plot is presented in Fig. 2, which compares SODA temperature data with observational data (Sedwick et al., 2008) (note the different colour scales). SODA

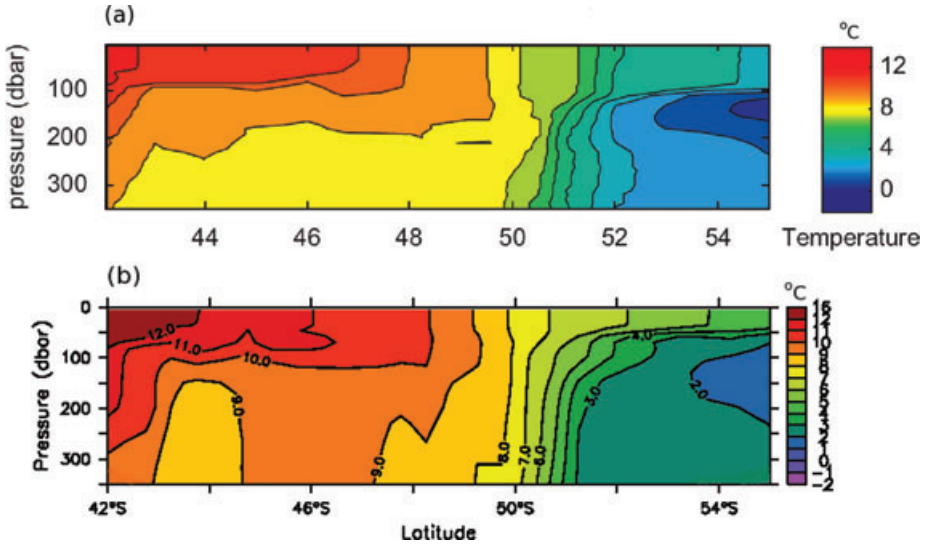

Fig. 2. Temperature distributions in March 1998 along 140°E from (a) (Sedwick et al., 2008, reprinted with permission from Elsevier) and (b) SODA. (Note the different colour scales).

temperature data is a very good match for the observational data, except perhaps near 44°S. Figure 3 shows a section, from 50 to 55°S, of the temperature plot in Fig. 2b, overlaid with isopycnals that represent UCDW. Note that UCDW is mainly found deeper than 350 m and south of the Polar Front (Johnston and Gabric, 2010), which is around 54°S here (Sedwick et al., 2008). Part (b) of the same figure is observational data for dissolved iron concentration (Sedwick et al., 2008), measured at the same time as the hydrographic data. By comparing the contours that delineate UCDW with the iron concentrations, it can be seen that UCDW coincides with a region of higher (around 0.3 nM) dissolved iron concentration values.

2.3. *Time series analyses*

The Australian sector from 110–160°E to 40–70°S is divided latitudinally into 5° zones, over which spatial averages for the various variables are computed. Temporal averages are computed

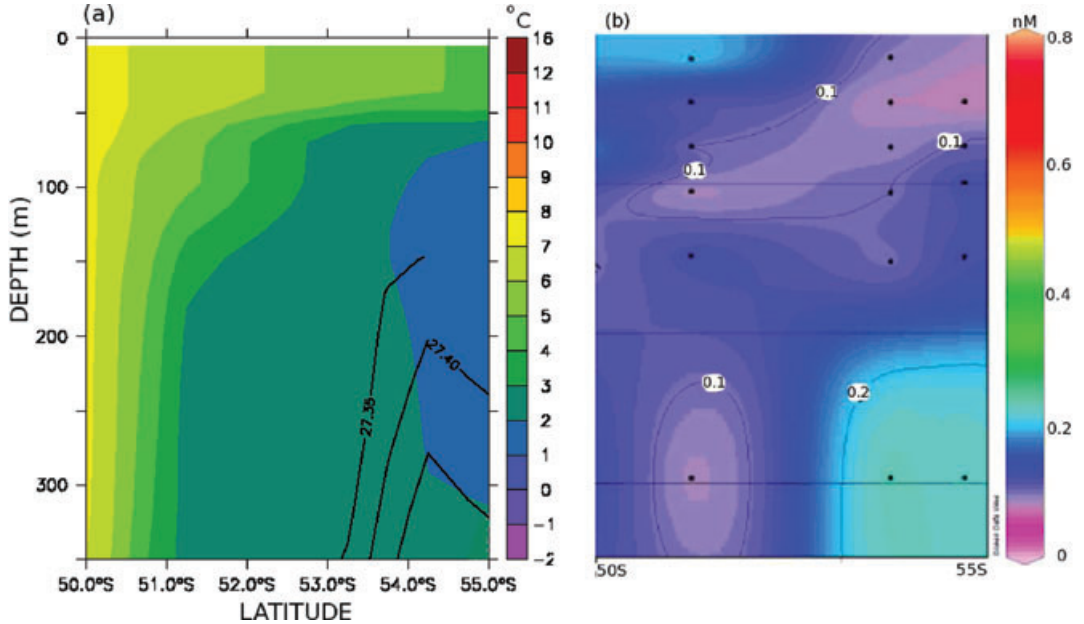

Fig. 3. (a) Temperature distribution in March 1998 along 140°E from SODA, overlaid with isopycnals identifying UCDW. Part (b) shows dissolved iron concentrations (Sedwick et al., 2008, reprinted with permission from Elsevier) measured at the same time as the temperatures shown in part (a). The isopycnals identifying UCDW coincide with higher values of dissolved iron.

at monthly and seasonal (where the calendar year is divided into four sets of three months, DJF, MAM and so on) scales. Since the majority of primary production occurs in spring and summer in the Southern Ocean, we focus on those two seasons. Climatologies are produced from medians of the monthly time series.

Mixed layer depths are calculated in SODA using the criterion of an absolute temperature difference of 0.2°C from the surface (Montegut et al., 2004). Examination of an alternative definition for MLD, using the density criterion of a 0.125 kg m^{-3} change in the potential density from the ocean surface (Monterey and Levitus, 1997), found that it made no difference to the types of trends found to be significant.

UCDW variables considered are the top depth where UCDW can be identified and the most southerly position where UCDW can be identified. Mean wind stress is calculated as the magnitude of the SODA wind stress vector $\boldsymbol{\tau} = (\tau_x^2 + \tau_y^2)^{\frac{1}{2}}$, from the SODA values for zonal and meridional wind stress, respectively, averaged over each latitudinal zone.

Other variables considered include stratification at the base of the mixed layer, which is calculated using the Brunt-Vaissala Frequency squared (N^2),

$$N^2 = -\frac{g}{\rho_0}\frac{\partial \sigma_\theta}{\partial z}, \tag{2}$$

where g is the acceleration due to gravity and ρ_0 is the average density for the zone. In addition the Ekman pumping rate, E, is defined as

$$E = -curl\left(\frac{\boldsymbol{\tau}}{\rho_0 f}\right), \tag{3}$$

where f is the Coriolis parameter. Related to the Ekman pumping rate is the northward Ekman transport, Q_E, which can be calculated as

$$Q_E = -\frac{X\tau_x}{\rho_0 f} \tag{4}$$

where X is the east–west distance across which the transport is calculated.

2.4. Climate indices

Indices to measure the SAM, prior to the satellite era (1979), have been constructed by Marshall (2003) and also Visbeck (2009) using Southern Hemisphere atmospheric pressure observations from stations situated either near 40°S or 65°S. Positive values of the SAM index indicate lower than normal atmospheric pressures over the polar regions, while negative values mean the opposite (that is, higher than normal pressures over the polar regions). The index constructed by Marshall (2003), chosen because both seasonal and annual values are available, is shown in Fig. 4 for summer for the period 1958–2007, along with the MEI and PDO Index.

The MEI (Wolter, 1987; Wolter and Timlin, 1993) is based on observations of sea level pressure, zonal and meridional surface wind components, SST and total cloudiness fraction of the sky, taken over the tropical Pacific. The MEI values are calculated as the first unrotated principal component of all these fields combined, computed for 12 sliding bi-monthly periods (that is, December/January, January/February and so on) and then standardized with respect to each season and to the 1950–1993 reference period. For seasonal correlation purposes, summer is taken to be November/December, December/January, January/February. Positive values of the MEI represent the warm ENSO phase (El Niño).

The PDO (Mantua and Hare, 2002) is a pattern of SST anomalies in the subtropical North and South Pacific, that are out of phase with SST anomalies in the tropical Pacific (Martinez et al., 2009). The PDO is defined (Mantua and Hare, 2002) as the leading empirical orthogonal function (EOF) of mean November through March SST anomalies for the Pacific Ocean north of 20°N latitude. For the EOF calculation, the global mean SST anomaly is first removed for each month in order to reduce the influence of the long-term trends in the data. Positive values indicate months of above normal SSTs along the west coast of North and Central America and on the equator, and below normal SSTs in the central and western north Pacific at about the latitude of Japan.

2.5. Statistical analyses

In order to examine the effect of the various variables considered in this study on biological productivity, correlations are computed between the variables and both chlorophyll-*a* and primary productivity. The variables considered include a number of climate indices, such as SAM, MEI and PDO, as well as sea-ice concentration, PAR and the SODA-derived variables discussed in Section 2.2.3. Correlations, using the Pearson correlation coefficient, are found using the 30 point seasonal time series, after detrending. Using these results and the R Statistical and Computing Package (R Foundation for Statistical Computing, Vienna, Austria), a multiple linear regression model is fitted between chlorophyll-*a* and those variables that are not correlated with one another.

Trends and their significance in seasonal (summer and spring) time series are estimated using the non-parametric seasonal Sen slope (Gilbert, 1987), a generalization of Sen's estimator of slope, and the seasonal Kendall test (Hirsch et al., 1982), a generalization of the Mann-Kendall test, which is not affected by seasonal cycles in the data. The non-parametric estimate of the slope is preferable to linear least squares regression due to its insensitivity to outliers (Gilbert, 1987; Hess et al., 2001). The test involves computing the Mann–Kendall test statistic and its variance separately for each month ('season'), with the data collected over years, and then summing these seasonal statistics to produce a Z statistic (Gilbert, 1987). Here the test is applied

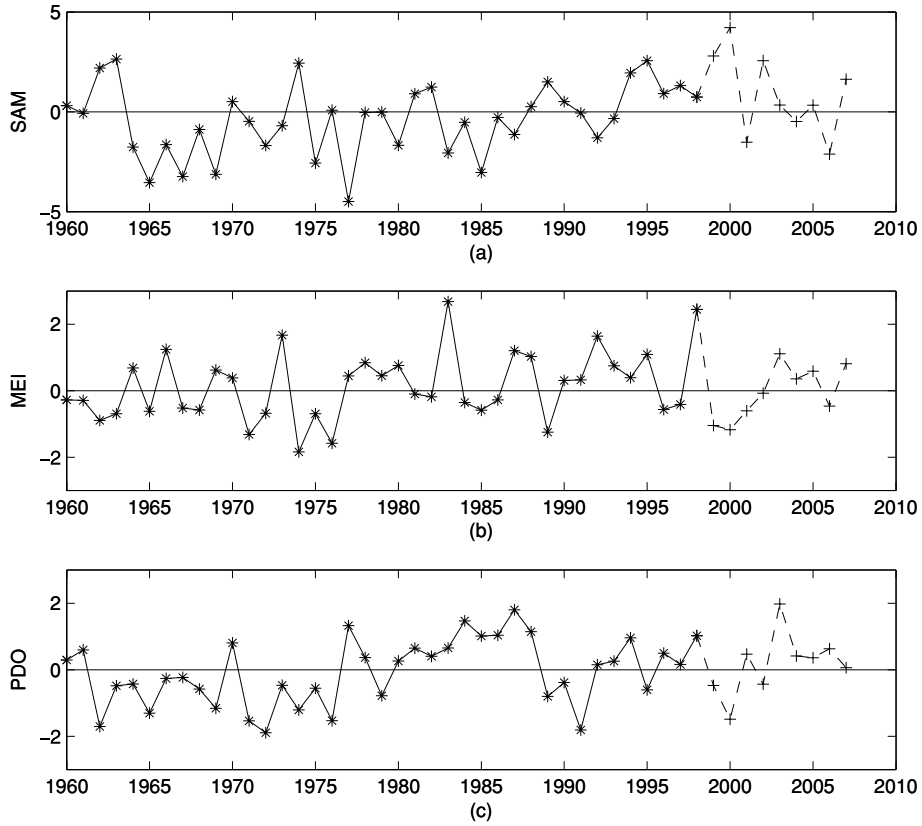

Fig. 4. Summer time series for (a) SAM (Marshall, 2003), (b) MEI (Wolter and Timlin, 1993) and (c) PDO (Mantua and Hare, 2002). The SAM time series shows a positive trend (increased wind stress) from the 1970s to the mid-1990s and a generally negative, but not significant, trend for the period (1998–2007) considered in this work. The 1998–2007 trends for MEI and PDO are also not significant. Positive MEI values represent the warm ENSO phase (El Niño) and positive PDO values represent months where there are above normal SSTs along the west coast of North and Central America and on the equator, and below normal SSTs in the central and western north Pacific.

to the time series for each month within a particular seasonal time series (e.g. summer) of 30 points, comprised of 10 yr worth of 3 months of data. The seasonal Sen's slope is then used to estimate a linear trend. Trends at the 95% confidence level are reported here as 'significant'.

3. Results and Discussion

3.1. Chlorophyll-a and primary productivity

Mean January (1998–2007) chlorophyll-*a* and estimated primary productivity (VGPM) are shown in Fig. 1 (where slight differences in the Antarctic coastline between the plots are due to the different masks applied). There are high chlorophyll-*a* values (around 0.5 mg m^{-3}) to the east of Tasmania, with the highest values (some in excess of 1 mg m^{-3}) near the Antarctic continent. The considerable interannual variation in chlorophyll-*a* is demonstrated in Fig. 5 for each of the six zones over the period September 1997 to August 2007. Peak chlorophyll-*a* values are generally around 1 mg m^{-3}, although the values for 2000 and 2002 are 2 and 3 times that, respectively. Peak chlorophyll-*a* values in the 65–70°S zone generally occur in December or January, after the 60–65°S zone where maximum values are usually in November. However in 60–65°S the 2000, 2002 and 2007 peaks are in January, December and December, respectively, corresponding to extreme values of around 0.6 mg m^{-3} in each case, compared with the usual peaks of 0.4 mg m^{-3} or less. During 1997–2007, peak values in the 50–55°S zone were in the range 0.2–0.3 mg m^{-3} and appear to be decreasing with time. Further north, chlorophyll-*a* values increase again with peaks up to 0.4 and 0.5 mg m^{-3} for 45–50°S and 40–45°S, respectively. These peaks occur anywhere between November and January for 50–55°S and November and February for 40–50°S, illustrating the interannual variability in phenology as well as in the magnitude of the bloom.

In contrast to chlorophyll-*a*, estimated primary productivity generally increases to the north (Fig. 1, Table 1). The exception to this is the 65–70°S zone in December, January and February, where primary productivity is higher than in 60–65°S and 55–60°S. This is consistent with high chlorophyll-*a* near the

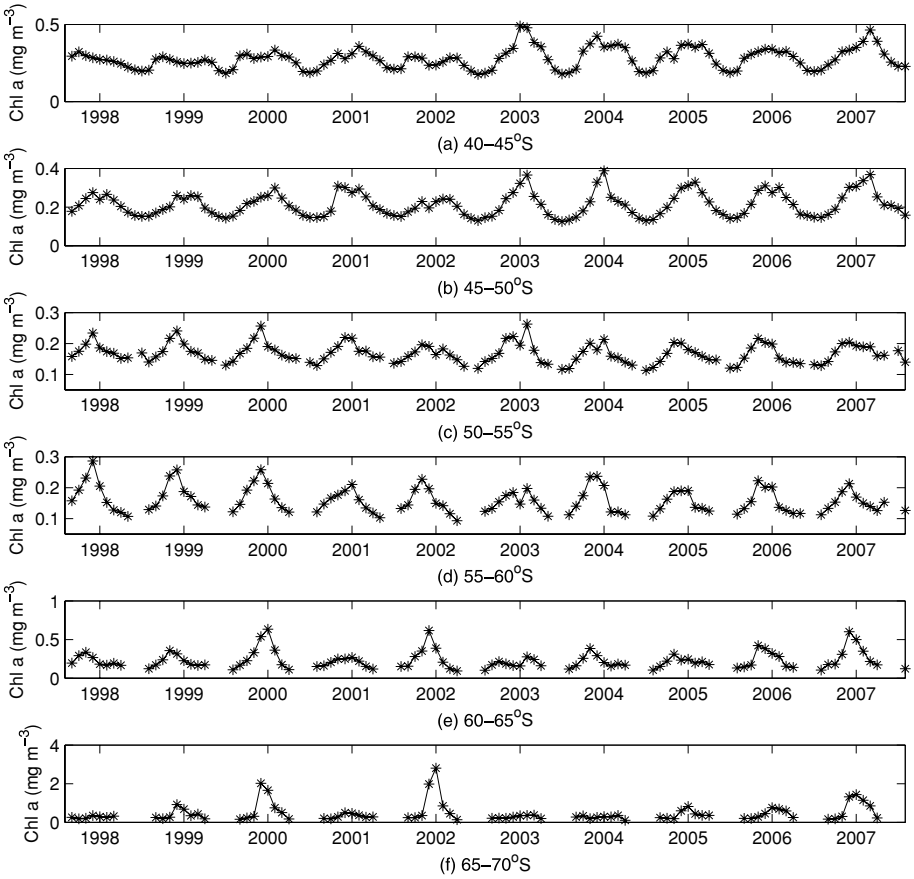

Fig. 5. Chlorophyll-*a* time series for September 1997-August 2007 for the (a) 40–45°S, (b) 45–50°S, (c) 50–55°S, (d) 55–60°S, (e) 60–65°S and (f) 65–70°S zones. Winter values are missing, which means that the time series starts again in July for (c), August for (d) and (e) and in September for (f). The tick mark is for January of the year indicated. Note the different vertical scales.

Antarctic shelf, due possibly to nutrients on the shelf but not the upwelling of nutrients, since UCDW is not found south of the Southern Boundary of the ACC (∼ 65°S).

Strong correlations are found between chlorophyll-*a* and primary productivity (0.75–0.97), in both spring and summer in all zones, except for spring in the 65–70°S zone (0.42) (Table 2).

3.2. Controls on chlorophyll-a and primary productivity

This section will focus on the main factors, found in Tables 3 and 4, that influence chlorophyll-*a* and primary productivity in the Southern Ocean. It should be noted that no correlations were found between chlorophyll-*a* or primary productivity and the MEI or the southern-most position of UCDW.

3.2.1. Sea-ice concentration. Little or no sea-ice is found north of 60°S and sea-ice concentrations of approximately 86 and 60%, for the 65–70°S and 60–65°S zones in spring, reduce to 70 and 32% in summer (Table 1). Interannual variability in sea-ice concentration in summer in the 65–70°S zone is shown in Fig. 6, in addition to decreases in sea-ice concentration which correspond to increases in chlorophyll-*a* and vice versa. Sea-ice concentration is an important factor in controlling the levels of chlorophyll-*a* (Table 3), in agreement with previous studies in this sector (Sokolov, 2008), including the inverse nature of the relationship. There are also similar correlations between primary productivity and sea-ice concentration (Table 4).

3.2.2. PAR. Climatological values for PAR are given in Table 1, where PAR is shown to increase northwards, except in spring in the most southerly zone, where the value of PAR is higher in the 65–70°S zone than in 55–65°, due to decreased cloud cover (Sokolov, 2008). Light availability has been suggested as one of the major controls on primary productivity in the Southern Ocean (Moore and Doney, 2006). Here, PAR was found to be highly positively correlated with chlorophyll-*a* in spring (0.82–0.94, except for 0.55 in 40–45°S, Table 3) and primary productivity in spring (0.94–0.98, Table 4), when the region is light-limited. These correlations are found for all zones except 65–70°S, where values for PAR are generally not available between May and September, so that in this case there is no SON time series. PAR is also positively correlated with chlorophyll-*a* (50–60°S) and primary productivity (50–65°S) in summer.

Table 1. Climatological values for Austral spring and summer by latitudinal zone (n/a = not applicable)

	65–70°S	60–65°S	55–60°S	50–55°S	45–50°S	40–45°S
Chlorophyll-*a* (mg m^{-3})[a]						
Summer	0.79	0.31	0.19	0.20	0.27	0.36
Spring	0.23	0.24	0.17	0.18	0.20	0.29
Primary productivity ($mgCm^{-2}d^{-1}$)[b]						
Summer	277.7	250.9	275.5	364.2	592.5	797.0
Spring	72.4	131.5	157.2	246.7	363.6	543.6
Mean wind stress (N m^{-2})[c]						
Summer	0.094	0.064	0.12	0.16	0.14	0.089
Spring	0.072	0.078	0.14	0.16	0.15	0.10
Sea-ice concentration(%)[d]						
Summer	69.8	31.7	n/a	n/a	n/a	n/a
Spring	86.4	59.9	n/a	n/a	n/a	n/a
PAR (Einst. m^{-2} d^{-1})[a]						
Summer	31.4	32.5	36.7	40.0	43.4	48.0
Spring	25.0	21.6	24.5	28.9	32.9	37.7
SST (°C)[c]						
Summer	−0.80	1.15	3.37	6.31	10.32	14.03
Spring	−1.40	−0.71	1.20	4.64	8.73	11.59
MLD (m)[c]						
Summer	86.9	38.7	35.4	48.9	55.4	30.5
Spring	117.4	71.8	88.1	124.0	152.5	112.4
Stratification (s^{-2})[c]						
Summer	2.8×10^{-5}	5.3×10^{-5}	5.3×10^{-5}	5.1×10^{-5}	5.9×10^{-5}	8.2×10^{-5}
Spring	1.7×10^{-5}	3.7×10^{-5}	3.4×10^{-5}	2.4×10^{-5}	2.3×10^{-5}	3.1×10^{-5}
Ekman transport (Sv)[c]						
Summer	n/a	0.98	2.7	4.5	4.8	3.2
Spring	n/a	1.4	3.0	4.3	4.7	3.8
Ekman pump rate (ms^{-1})[c]						
Summer	n/a	1.9×10^{-6}	1.1×10^{-6}	n/a	n/a	n/a
Spring	n/a	1.8×10^{-6}	0.67×10^{-6}	n/a	n/a	n/a
UCDW top depth (m)[c]						
Summer	n/a	41.3	52.1	108.8	346.8	1124
Spring	n/a	58.9	70.2	120.9	422.2	1112

[a]Source: SeaWiFS
[b]Source: VGPM
[c]Source: SODA
[d]Source: National Snow and Ice Data Center

Table 2. Correlations (significant at the 95% confidence level) between chlorophyll-*a* and primary productivity by latitudinal zone

	65–70°S	60–65°S	55–60°S	50–55°S	45–50°S	40–45°S
Summer	0.89	0.75	0.81	0.86	0.79	0.94
Spring	0.42	0.90	0.92	0.97	0.96	0.77

3.2.3. SST. Climatological values for summer and spring SST (Table 1) increase to the north, with spring values lower than summer values. Results of correlations between chlorophyll-*a* or primary productivity and SST, (Tables 3 and 4, respectively) show that, in summer, there is a negative correlation between SST and both chlorophyll-*a* (50–65°S) and primary productivity (60–65°S), whereas in spring (40–60°S) there is a positive relationship. No significant correlations between SST and chlorophyll-*a* and primary productivity are found in 65–70°S in either season. The difference between the direction of the correlations in spring and summer may be related to the fact that in spring increasing temperature leads to increasing ice melt, which

Table 3. Correlations (significant at the 95% confidence level) between various variables and chlorophyll-*a*, by latitudinal zone and season, in decreasing order. PAR values for 65–70°S are not available in spring. Abbreviation of variable names is as follows: Sea-ice conc = Sea-ice concentration, Mean WS = Mean wind stress, Strat = Stratification, Top UCDW = Top UCDW depth, Ek Pump/Trans = Ekman pumping rate/transport

65–70°S	60–65°S	55–60°S	50–55°S	45–50°S	40–45°S
		Summer			
Sea-ice conc (–0.65)	PDO (–0.67)	PAR(0.70)	PAR (0.44)		PDO (0.47)
PDO (–0.58)	SST (–0.66)	SST(–0.61)	SST (–0.39)		Strat (0.42)
SAM (0.48)	Strat (–0.60)	Strat(–0.47)			
	Mean WS (0.55)				
	Ek Trans (0.47)				
	Top UCDW (0.39)				
		Spring			
Sea-ice conc (–0.53)	PAR (0.82)	PAR (0.90)	PAR (0.94)	PAR (0.86)	PAR (0.55)
	Sea-ice conc (–0.69)	SST (0.59)	MLD (–0.74)	SST (0.82)	MLD (–0.56)
		MLD (–0.58)	SST (0.70)	Strat (0.69)	Strat (0.42)
		Ek Pump (–0.37)	Strat (0.47)	MLD (–0.68)	SST (0.37)
			Mean WS (–0.41)		
			Ek Trans (–0.40)		

Table 4. Correlations (significant at the 95% confidence level) between various variables and primary productivity, by latitudinal zone and season, in decreasing order. PAR values for 65–70°S are not available in spring. Abbreviation of variable names is as follows: Sea-ice conc = Sea-ice concentration, Mean/Max WS = Mean/Maximum wind stress, Strat = Stratification, Ek Pump/Trans = Ekman pumping rate/transport

65–70°S	60–65°S	55–60°S	50–55°S	45–50°S	40–45°S
		Summer			
PDO (–0.57)	SST (–0.52)	PAR (0.82)	PAR (0.70)		Strat (0.45)
SAM (0.48)	PAR (0.50)	MLD (0.39)			
Sea-ice conc (–0.45)	Top UCDW (0.45)				
	PDO (–0.44)				
		Spring			
Sea-ice conc (−0.81)	PAR (0.96)	PAR (0.98)	PAR (0.98)	PAR (0.95)	PAR (0.94)
Strat (0.51)	Sea-ice conc (−0.79)	SST (0.79)	MLD (−0.76)	SST (0.82)	MLD (−0.84)
Max WS (−0.38)	Ek Pump (−0.47)	MLD (−0.70)	SST (0.73)	MLD (−0.71)	SST (0.77)
	SST (0.38)	Max WS (−0.38)	Strat (0.51)	Strat (0.43)	
	Max WS (−0.37)		Max WS (−0.43)	Mean WS (−0.39)	
			Mean WS (−0.43)	Ek Trans (−0.36)	
			Ek Trans (−0.41)		

leads both to increased iron being released as well as to the formation of shallower mixed layers, both of which are related to increases in chlorophyll-*a* and primary productivity. However, in summer in 50–60°S where chlorophyll-*a* is low (see Table 1), increasing SST may not increase chlorophyll-*a* if nutrients such as iron are limiting (de Baar et al., 2005).

3.2.4. Mixed layer depth and stratification. The depth of the mixed layer (Table 1) varies between latitudinal zones and seasons. Deeper mixed layers occur in spring than in summer and the mixed layer generally shallows towards the Antarctic continent, except for the most northerly zone and 65–70°S, which are both exceptions. Negative correlations, between MLD and both chlorophyll-*a* and primary productivity, are found in spring for all but the two southern-most zones (Tables 3 and 4). These results are consistent with previous studies (Mitchell and Holm-Hansen, 1991; de Baar et al., 2005), indicating that as the mixed layer deepens, chlorophyll-*a* decreases (due to light limitation). Interestingly, no significant correlations are found in summer between MLD and chlorophyll-*a*, and only one between MLD and primary productivity. This would seem to indicate that mixed layers are already sufficiently shallow in summer.

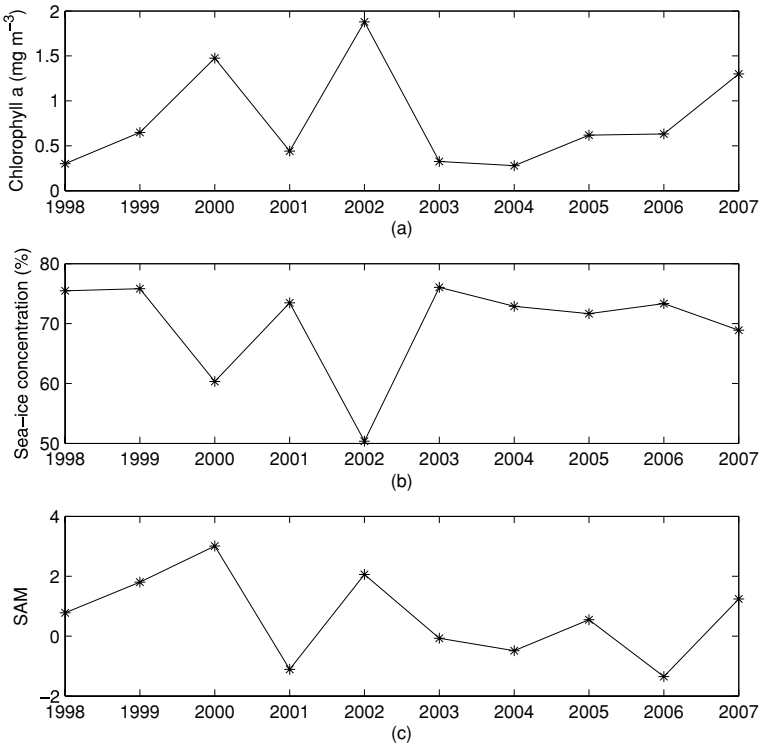

Fig. 6. Summer time series for 1998–2007 in sector (110–160°E, 65–70°S) for (a) Chlorophyll-*a*, (b) Sea-ice concentration and (c) SAM.

Climatological values for stratification in summer, also given in Table 1, generally increase to the north. However, in spring, the highest value is in the 60–65°S zone, north of which stratification decreases, except in the most northerly zone. Stratification is higher in summer than in spring in all cases, generally by a factor of 1.5–2.5, due to higher temperatures, sea-ice melt and lower wind stress. Positive correlations are found between stratification and both chlorophyll-*a* and primary productivity in spring in 40–55°S and summer in 40–45°S (Tables 3 and 4). The opposite is true for the only other correlation between stratification and chlorophyll-*a* in summer though, which occurs in 60–65°S, a region of low wind stress in summer (Table 1), where decreased stratification (and increased mixing of nutrients) may be related to an increase in chlorophyll-*a*.

3.2.5. PDO. A number of significant correlations are found between the PDO and both chlorophyll-*a* and primary productivity (Tables 3 and 4), but only in summer. The sign of the correlations is negative in 60–70°S and positive in 40–50°S. The fact that there are correlations between chlorophyll-*a* and PDO is consistent with work by Martinez et al. (2009) who have recently shown that multi-decadal changes in global phytoplankton abundance can be related to basin-scale oscillations of the physical ocean (i.e. the PDO in this region), by examining the covariability of chlorophyll-*a* and SST.

3.2.6. Comparison of controls on chlorophyll-a with controls on primary productivity. As would be expected from the form of Equation (1), significant correlations are found between primary productivity and chlorophyll-*a*, PAR, MLD and SST (Tables 2 and 4). Interestingly, the modelled primary productivity is also correlated with sea-ice concentration, stratification and mean and maximum wind stress, which are not represented explicitly in the model. A comparison of Tables 3 and 4 shows very similar results for correlations of factors with either chlorophyll-*a* or primary productivity. In the more detailed analysis to follow the work will focus on correlations with chlorophyll-*a*, given the various caveats associated with the modelling of primary productivity.

3.3. Controls on Chlorophyll-a by Zone

3.3.1. Spring. Based on the results from Table 3, the important factors that influence chlorophyll-*a* in the Southern Ocean during spring are: sea-ice concentration in 60–70°S (negative correlation); PAR, which is highly positively correlated across all zones, except 65–70°S where September data is missing; SST (positive correlation) and MLD (negative correlation) for 40–60°S and stratification (positive correlation) for 40–55°S. It should be noted, however, that many of these factors covary. Some (lower-valued) correlations are also found in 50–55°S between chlorophyll-*a* and Ekman transport and mean wind stress and in 55–60°S between chlorophyll-*a* and Ekman pumping rate. Interestingly, these correlations are negative in each case, indicating an increase in chlorophyll-*a* associated with a decrease in the other variable. In the case of mean wind stress this may indicate that increased chlorophyll-*a* is related to reduced

mixing of phytoplankton away from available light, given the importance of light in spring. However, it is unclear why the are negative correlations between chlorophyll-*a* and the Ekman variables.

3.3.2. The 65–70°S zone in summer. In the 65–70°S zone, significant correlations exist between chlorophyll-*a* and sea-ice concentration (negative), PDO (negative) and SAM (positive) (Table 3). However, since no correlation was found between SAM and sea-ice concentration, in contrast to PDO and sea-ice concentration, which were found to be correlated, this work will concentrate on the former variables. Examination of the time series for chlorophyll-*a*, sea-ice concentration and SAM in Fig. 6 indicates that the maximum chlorophyll-*a* values in 2000 and 2002 coincide with low sea-ice concentration and high SAM values. Using a multivariate linear regression model it is found that sea-ice concentration and SAM together can explain 51% of the variance in chlorophyll-*a*.

3.3.3. The 60–65°S zone in summer. The largest list of factors affecting chlorophyll-*a* in summer is found for the 60–65°S zone in summer: PDO, SST and stratification (negatively correlated); mean wind stress, northward Ekman transport and UCDW top depth (positively correlated). Since nutrient-rich UCDW upwells between the Polar Front and the Southern Boundary of the ACC and then moves northward under Ekman transport, it seems worthwhile to investigate these connections, despite the fact that the correlations are relatively low. Many of the factors in the list above covary (for example, stratification is affected by SST and mean wind stress) and only SST and mean wind stress are found to be uncorrelated. The time series for these two variables, as well that for chlorophyll-*a* (Fig. 7), show that high chlorophyll-*a*, again in 2000, 2002 and 2007, is related to high mean wind stress occurring at the same time as low SST. In this case, SST and mean wind stress together account for 55% of the variance in chlorophyll-*a*.

The positive correlation between UCDW top depth and chlorophyll-*a* is interesting, in that it implies that when UCDW is not advected as close to the surface, chlorophyll-*a* increases. A negative correlation is found between UCDW top depth and SST; that is, when UCDW is nearer to the surface, SST increases (and chlorophyll-*a* decreases). In summer in the 60–65°S zone, the climatological value for SST is around 1.2°C (Table 1), while the UCDW temperature is around 1.9°C (Johnston and Gabric, 2010). This is consistent with UCDW nearing the surface having a warming effect on SST, as indicated above. However, this is clearly not the whole story, firstly, because these two factors do not explain all the variance in chlorophyll-*a* and secondly, because UCDW carries nutrients that are essential for primary production. We hypothesize that favourable conditions for phytoplankton growth, in summer in the 60–65°S zone, involve high wind stress to mix these nutrients into the mixed layer, combined with low SST (Fig. 7). Iron sources could include both UCDW, which intrudes into the mixed layer mainly in summer and autumn in this zone (Fig. 8), as well as the melting sea-ice, since a significant correlation between sea-ice concentration in the

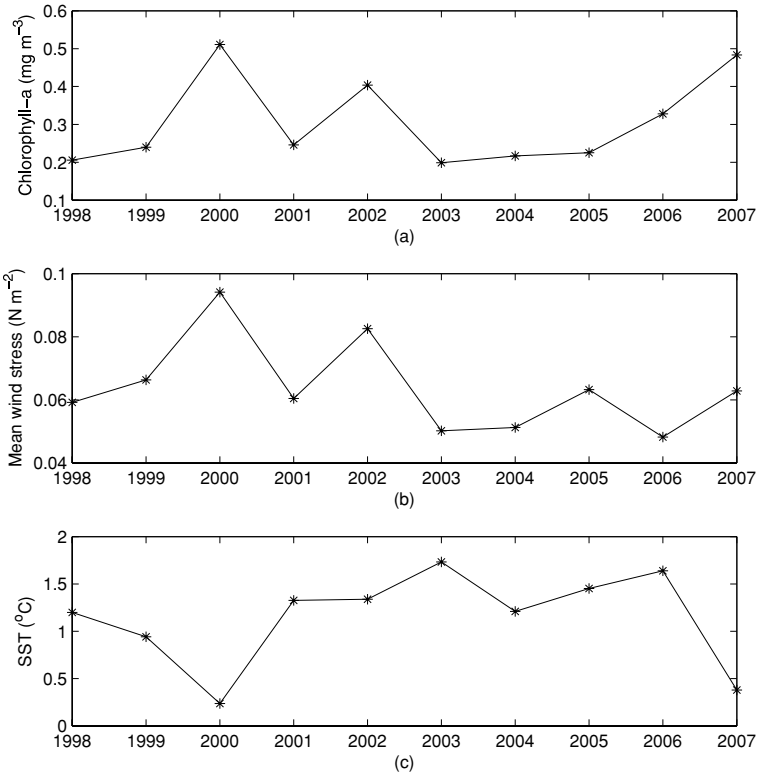

Fig. 7. Summer time series for 1998–2007 in sector (110–160°E, 60–65°S) for (a) Chlorophyll-*a*, (b) Mean wind stress and (c) SST.

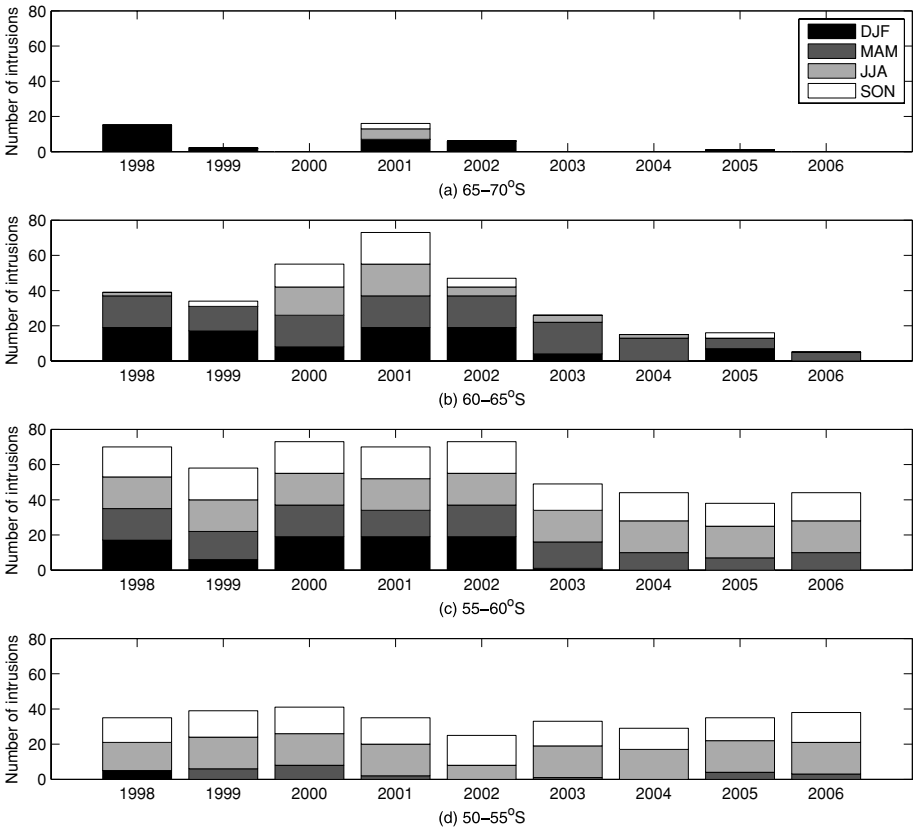

Fig. 8. Number of times that UCDW is entrained in the mixed layer by season and year in (a) 65–70°S, (b) 60–65°S, (c) 55–60°S and (d) 50–55°S.

previous spring and chlorophyll-*a* in the following summer is also found (not presented).

3.3.4. The 50–55°S and 55–60°S zones in summer. Both PAR (positive correlation) and SST (negative correlation) are significant factors affecting chlorophyll-*a* in 50–60°S in summer, in addition to stratification in 55–60°S (Table 3). Again, as in spring, these factors covary.

3.3.5. The 40–45°S and 45–50°S zones in summer. None of the factors considered here was found to be significantly correlated with chlorophyll-*a* in the 45–50°S zone. However, PDO and stratification were both positively correlated with chlorophyll-*a* in the 40–45°S zone (Table 3), in contrast to the negative correlations found between these variables and chlorophyll-*a* further south. Both of these regions can be impacted by mineral dust deposition from the Australian continent (Gabric et al., 2010) and this is consistent with the large interannual variability in the phenology and magnitude of the bloom (Fig. 5).

3.4. Trends over the Period 1997–2007

Before studying trends over the period 1997–2007, it is worth noting that the SAM does not display a positive trend in summer and autumn over this time (Monaghan et al., 2008), in contrast to the trend from the 1970s to the late 1990s (Thompson and Solomon, 2002). The SAM index for summer for 1958–2007 is shown in Fig. 4 and the negative trend for 1997–2007 in summer is found to be significant only at the 90% confidence level, whereas the trend for spring is not statistically significant. No trends were found for the PDO index, while the MEI had a positive trend in spring only.

3.4.1. Trends in satellite and SODA-derived variables. In addition to trends in chlorophyll-*a* and primary productivity, trends in all the variables identified in Section 2 as possibly affecting chlorophyll-*a* or primary productivity are presented in Table 5 for completeness. Sea-surface salinity (SSS) is also presented, although it was not included in the previous section as it is only an indirect control through its effect on stratification. No trends in summer or spring were found for PAR or the southernmost position of UCDW. Previous work by Johnston and Gabric (2010) analysed trends in hydrodynamic variables similar to those here, in the same region but over the longer time period 1958–2005, and when the SODA-derived trends from Table 5 are compared with those, two differences are apparent. One is that the 1997–2007 trends are generally about an order of magnitude larger than the 1958–2005 trends and the second is that the sign of the trends is very often opposite to that for the longer time period.

Table 5. Trends (per year) for September 1997 to August 2007 by latitudinal zone for Austral spring and summer. Blanks mean no significant trend was found (n/a = not applicable). No significant trends were found for PAR, SAM, PDO or southern-most position of UCDW

	65–70°S	60–65°S	55–60°S	50–55°S	45–50°S	40–45°S
Chlorophyll-*a* (mg m^{-3} yr^{-1})						
Summer			-2.7×10^{-3}		7.2×10^{-3}	1.2×10^{-2}
Spring			-2.7×10^{-3}			
Primary productivity (mg C $m^{-2}d^{-1}$ yr^{-1})						
Summer					8.4	14.7
Spring						
Mean wind stress (Nm^{-2} yr^{-1})						
Summer			-3.7×10^{-3}	-8.3×10^{-3}	-5.5×10^{-3}	
Spring	-8.7×10^{-3}	-5.7×10^{-3}	-1.4×10^{-2}	-1.4×10^{-2}	-5.8×10^{-3}	-4.6×10^{-3}
Sea-ice concentration (% yr^{-1})						
Summer			n/a	n/a	n/a	n/a
Spring	−0.31		n/a	n/a	n/a	n/a
SST (°C yr^{-1})						
Summer		4.3×10^{-2}	9.5×10^{-2}	6.7×10^{-2}		-4.5×10^{-2}
Spring	-3.3×10^{-2}	-5.4×10^{-2}	4.9×10^{-2}	5.7×10^{-2}		
SSS (yr^{-1})						
Summer		-2.0×10^{-2}		2.5×10^{-2}	4.0×10^{-2}	2.6×10^{-2}
Spring	-8.9×10^{-3}	-2.4×10^{-2}		2.3×10^{-2}	4.1×10^{-2}	2.0×10^{-2}
Mixed layer depth (m yr^{-1})						
Summer		−2.4				
Spring	−7.3					
Stratification (s^{-2} yr^{-1})						
Summer				-2.6×10^{-6}	-4.1×10^{-6}	
Spring	9.0×10^{-7}		-3.1×10^{-6}	-2.0×10^{-6}	-1.9×10^{-6}	
Ekman transport (Sv yr^{-1})						
Summer	n/a		-7.7×10^{-2}	-2.3×10^{-1}	-1.7×10^{-1}	
Spring	n/a		-3.0×10^{-1}	-3.5×10^{-1}	-1.7×10^{-1}	-1.9×10^{-1}
Ekman pumping ($ms^{-1}yr^{-1}$)						
Summer	n/a			n/a	n/a	n/a
Spring	n/a	-1.7×10^{-7}		n/a	n/a	n/a
UCDW top depth (m yr^{-1})						
Summer	n/a	6.0	13.4	7.7		
Spring	n/a	5.0	12.0	8.4		

In order to compare these 1997–2007 trends with previous trends over longer time periods, plots of 'running' trends are produced, similar to plots for SAM by Monaghan et al. (2008), for each latitudinal zone and season, for the various SODA-derived variables presented in Table 5. The trends are calculated from the start year to 2007, so that in Fig. 9 the value at 1958 represents the trend in summer SST from 1958 to 2007, while the final point is the trend for the time series, 1998–2007, considered in this study. The shaded areas show the 95% confidence interval for the trends and this increases as expected for later start years, where the time series is shorter. Note that start year varies between 1958 and 1998 for spring, whereas for summer it is 1959 to 1998, since the first summer season from December 1958 to February 1959 is labelled as 1959.

Figures 9 and 10 generally show quite stable initial trends for SST and SSS, respectively, followed by later either increasing or decreasing trends. These increasing or decreasing trends appear to be occurring, even allowing for the fact that the later time series are shorter and the confidence intervals are wider. There are strong recent increases in SST in 50–60°S in both spring and summer, with decreases north and south of there, except in 60–65°S in summer (Fig. 9). The difference between SSS trends in different latitudinal zones is illustrated in Fig. 10, where SSS trends are increasing north of 50°S and decreasing south of there, for start years of around 1980. When similar analyses are performed for the other SODA-derived variables presented in Table 5, for each latitudinal zone and season, there appears to have been a detectable change in the trends for many of the variables.

3.4.2. UCDW intrusions into the mixed layer. The vertical advection of nutrient-rich UCDW into the mixed layer is thought to be critical for primary productivity (Martin et al., 1990;

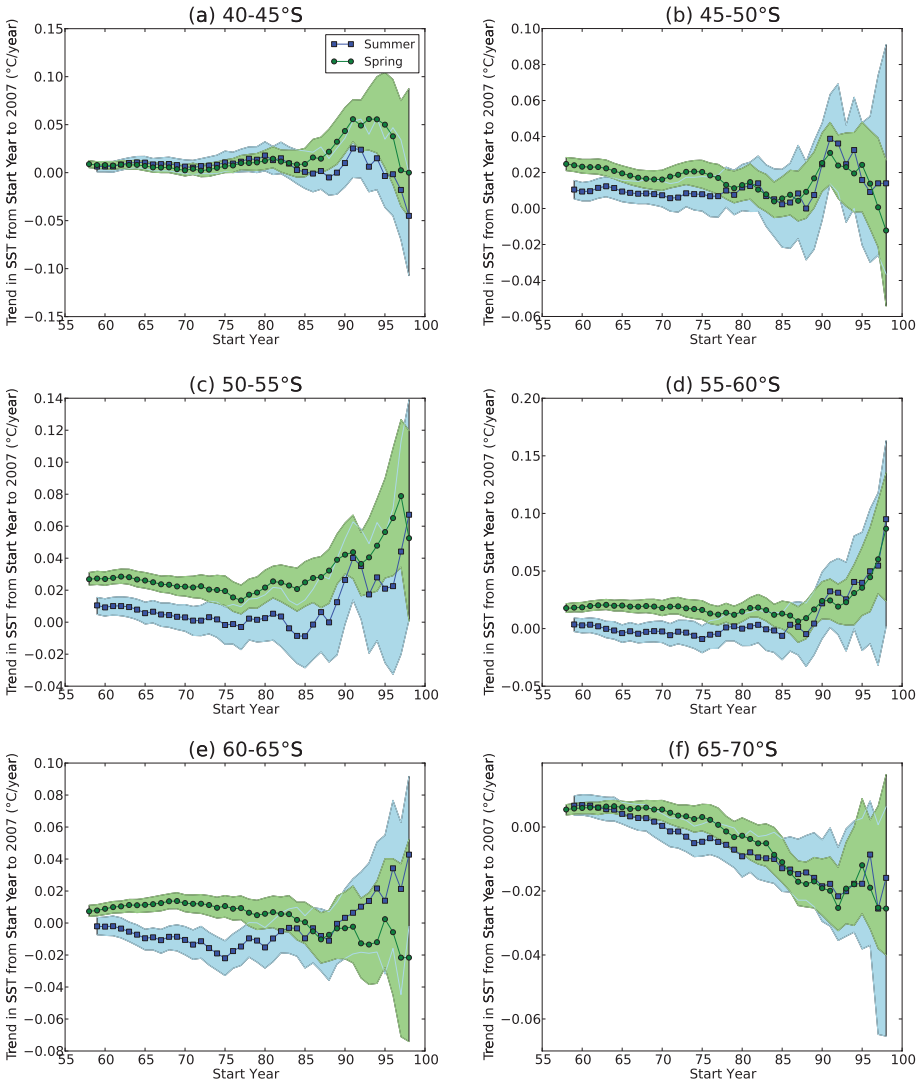

Fig. 9. Trends for Sea-surface Temperature for summer and spring, for the time series from the start year to 2007, with the 95% confidence intervals shaded.

Hoppema et al., 2003) and this may occur between the Polar Front and the Southern Boundary of the ACC. Here the frequency with which UCDW is entrained in the mixed layer is examined to see if any change has occurred over the period 1997–2007. Rather than using the SODA monthly data sets, here the SODA 5-d data sets (pentads) are used to analyse the frequency of intrusions on a finer time-scale. UCDW is deemed to have entered the mixed layer if the top position of UCDW (UCDW top depth) is shallower than the MLD at any particular gridpoint. Values for UCDW top depth and MLD in summer (Table 1) may be misleading in that they imply that UCDW does not upwell high enough to enter the mixed layer, but that is because they are climatological rather than actual values.

The number of times UCDW is entrained in the mixed layer is presented by season and year for each of the 5° latitudinal zones between 50 and 70°S in Fig. 8, where the 73 pentads in a year are recombined to form 'seasons', which consist of 18 pentads, except for December which contains an extra pentad. Fig. 8 shows that UCDW reaches the 65–70°S zone only in some years, depending on the position of the Southern Boundary of the ACC, and because of this, neither climatological values (Table 1) nor trends (Table 5) for UCDW top depth are given in this zone. UCDW is entrained in the 60–70°S zones predominantly in summer and autumn (Fig. 8), a situation that was also noted in the previous 1958–2005 work (Johnston and Gabric, 2010). In contrast in 55–60°S, UCDW is found in the mixed layer in all four seasons in 1998–2002 and mainly in autumn and winter in the 50–55°S zone. The overall figure is consistent with the upwelling of UCDW in 60–65°S in summer and autumn, followed by the movement north of this water by Ekman transport, which leads to larger numbers of intrusions in winter and spring in 55–60°S and 50–55°S.

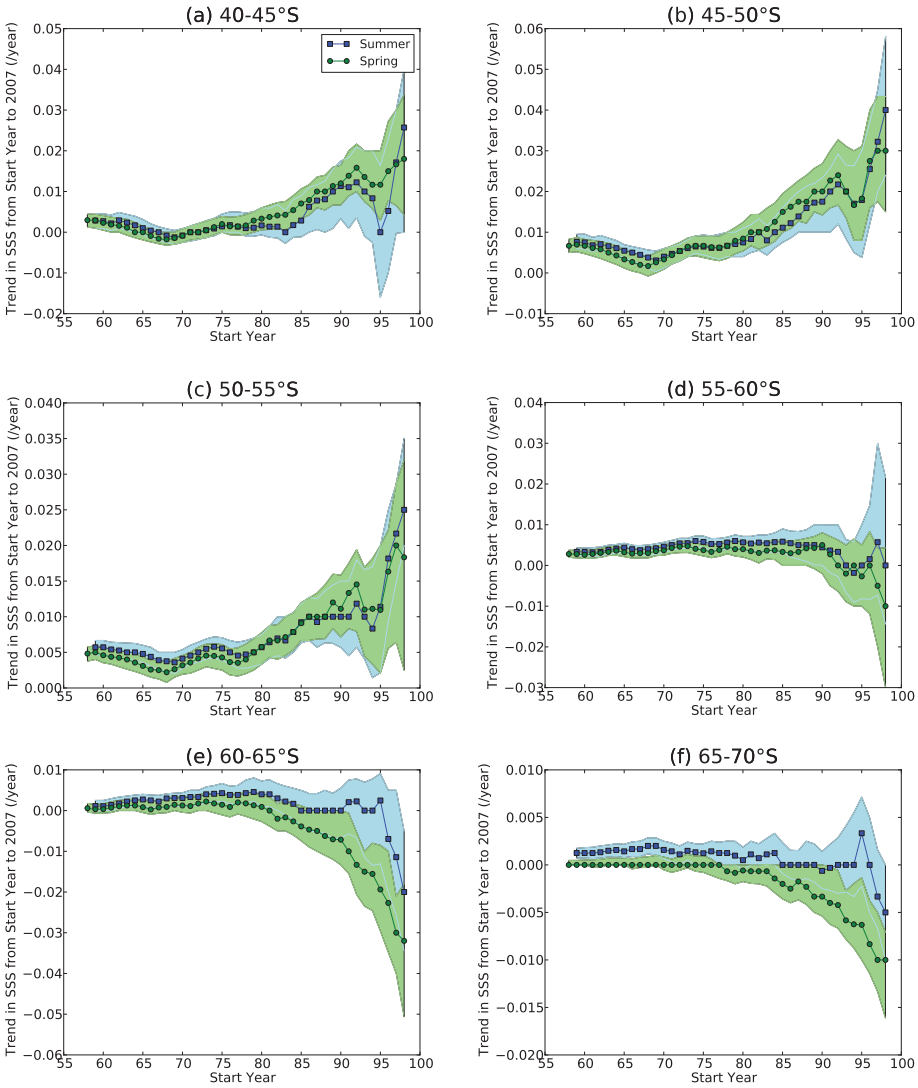

Fig. 10. Trends for Sea-surface Salinity for summer and spring, for the time series from the start year to 2007, with the 95% confidence intervals shaded.

In terms of temporal trends in the number of intrusions of UCDW into the mixed layer in summer and spring, which are the seasons of interest here, we find a statistically significant decrease in summer in the 60–65°S and 55–60°S zones. This does not seem to be the case, however, in spring. These results are consistent with trends found for UCDW top depth in summer in 60–65°S in Table 5 which show that UCDW is found further from the surface and the mixed layer is shallowing. Again, when our results are compared with the analysis for 1958–2005 in Johnston and Gabric (2010), the trend of a decreasing number of intrusions of UCDW in summer into the mixed layer in 1997–2007 is opposite to the trend for the longer time period.

3.4.3. Trends in chlorophyll-a and primary productivity. When the summer and spring time series for chlorophyll-*a* are examined for trends, negative trends in chlorophyll-*a* are found for both seasons in the 55–60°S zone and positive trends for both chlorophyll-*a* and primary productivity are found in summer in the two most northerly zones (40–50°S) (Table 5). These results are presented with the caveat that there is some uncertainty in primary productivity trends that are derived using surface chlorophyll-*a*, given that ocean colour models are more challenged to model short time-period trends (such as those considered here) than longer-period trends (Saba et al., 2010b).

The summer chlorophyll-*a* results are consistent with the work of Henson et al. (2010), who produced global maps of the trend in monthly anomalies in SeaWiFS chlorophyll-*a* for September 1997 to December 2007, which show, for the Australian sector, a

band of increasing chlorophyll-*a* around 40–45/50°S and a band of decreasing chlorophyll-*a* between about 45/50°S and 60°S, as well as small patches of increasing chlorophyll-*a* near the Antarctic continent. Since the trends in our work are presented by season and those of Henson et al. (2010) are annual trends, in order to make the comparison the assumption is made that, where there are opposite trends in summer and spring, the summer trends dominate, due to the larger values for summer both in chlorophyll-*a* and chlorophyll-*a* trends. Trends for primary productivity in summer are also similar to those found, for annual values, by Henson et al. (2010), who use primary productivity estimated from three different algorithms, one of which is the VGPM algorithm used here.

Positive trends are found for chlorophyll-*a* and primary productivity in the two most northerly zones 40–45°S and 45–50°S in summer (Table 5). However, further study is needed into the reasons for these trends, given that the only factors found here that correlate positively with chlorophyll-*a* are PDO and stratification in 40–45°S (Table 3) and stratification with primary productivity (Table 4). One factor that needs to be taken into account in these northern latitudes is the effect of mineral deposition of dust from the Australian continent, which can affect both the phenology and the magnitude of the bloom (Gabric et al., 2010). Significant negative trends are also found for chlorophyll-*a* in the 55–60°S zone in both summer and spring (Table 5). In summer, these trends are consistent with the positive trends found for SST (Table 5), in conjunction with the negative correlation between SST and chlorophyll-*a* (Table 3) in that zone. The fact that Ekman transport is also decreasing there, presumably with a concomitant decrease in the supply of iron, is also consistent with decreasing chlorophyll-*a*. However, SST cannot be the key factor in spring since the positive correlation between SST and chlorophyll-*a* (Table 5) then would suggest increasing not decreasing chlorophyll-*a*. In this case, a decrease in the Ekman transport as discussed above and a decrease in stratification (Table 5) may be relevant.

3.5. Comparison with other studies

3.5.1. Controls on chlorophyll-a and primary productivity. In their study of primary production in the Southern Ocean in 1997–2006, Arrigo et al. (2008) found that interannual production covaried with sea-ice cover, although changes in SST played a role. Our study agrees with those results, finding an inverse relationship between chlorophyll-*a* and sea-ice concentration, as pointed out for this region by Sokolov (2008), as well as the same relationship with primary production. Other studies have highlighted the importance of irradiance in the light-limited Southern Ocean (Smith and Comiso, 2008) and our work finds strong correlations between PAR and both chlorophyll-*a* and primary productivity in spring and in the 50–60°S zones in summer. However, no correlations between PAR and chlorophyll-*a* are found in summer in the two most southerly zones, which agrees with recent work by Venables and Moore (2010), who report that for at least 3 months of the year (summer), light limitation does not significantly constrain chlorophyll-*a* in High-Nutrient Low–Chlorophyll regions such as the region under study here.

The fact that chlorophyll-*a* is likely to be affected by MLD, stratification and SST has been shown in previous studies (Mitchell and Holm-Hansen, 1991; de Baar et al., 2005; Behrenfeld et al., 2006; Arrigo et al., 2008) and these were found to be important factors here, bearing in mind that they covary. However, no correlations were found here with MLD in summer, perhaps due to shallowing of the mixed layer in that season. The interesting thing about SST is that its correlation with chlorophyll-*a* is negative in summer, but positive in spring (a pattern that is repeated for stratification, apart from the 40–45°S value). Previous work has already identified an inverse relationship between chlorophyll-*a* and SST at interannual timescales (Behrenfeld et al., 2006; Martinez et al., 2009). In contrast, a recent study (Saba et al., 2010b) has found a positive relationship between the two at station HOT (Hawaiian Ocean Time-Series), where the authors found that surface fields, such as SST and chlorophyll-*a*, did not necessarily correlate well with the increase in integrated primary productivity, since the deep layer forcing was driving the increase. Also, Arrigo et al. (2008) found a complex relationship between primary production and SST, with positive correlations in some regions and negative correlations in others. They attribute this to the fact that SST affects primary production both directly (through the relationship between temperature and phytoplankton metabolic rate) and indirectly (through the effect of temperature on stratification and sea-ice). Our study also found correlations between the PDO and both chlorophyll-*a* and primary productivity in summer: positive in 40–45°S (chlorophyll-*a* only) and negative in both 60–65°S and 65–70°S. This is consistent with work by Martinez et al. (2009) who looked at the covariability of chlorophyll-*a* and SST over decadal timescales and concluded that the spatial pattern of the changes bore the imprint of the PDO.

Perhaps surprisingly, this study finds only one significant correlation between both chlorophyll-*a* and primary productivity and SAM (positive in the 65–70°S zone in summer). This is in contrast to a previous study (Lovenduski and Gruber, 2005), which used SeaWiFS 8-d data from 1997 to 2004 and considered zones based on climatological fronts and thus differed slightly from this study. The Lovenduski and Gruber (2005) study linked SAM to different variations in mid- and high-latitude primary production north and south of the Polar Front and suggested that the positive correlation of chlorophyll-*a* and SAM south of the Polar Front was related to an increased supply of iron during upwelling, while the negative correlation north of the Polar Front was because of stronger light limitation due to deeper mixed layers. However, the SAM-chlorophyll-*a* correlations in the study by Lovenduski and Gruber (2005) were actually only significant

in the Subantarctic zone south of Australia and elsewhere they were small and often not statistically significant. Arrigo et al. (2008) conclude that 31% of the variation in annual production in the Southern Ocean is explained by SAM, but again the result is not statistically significant. The short data record and the seasonal approach may explain the lack of significant correlations in our study also. In fact, our study does find a combination of (non-significant) positive (50–70°S) and negative correlations (40–50°S) between SAM and chlorophyll-*a* in summer, in agreement with Lovenduski and Gruber (2005). This includes one in the 60–65°S zone that is significant at the 94% confidence level and is likely to be related to other significant factors found in that zone, such as mean wind stress and northward Ekman transport. Finally, it should be noted that in spring all the SAM-chlorophyll-*a* correlations appear to be positive, indicating that different processes seem to be dominant in spring compared with summer.

When considering factors which affect chlorophyll-*a* it is worth noting the comments of Behrenfeld et al. (2009), who point out that correlations between SST and chlorophyll-*a* emerge because SST acts as a surrogate for other environmental factors (such as nutrients, including iron, and mixed layer light levels) that vary with SST and directly impact phytoplankton light levels. They also note that the relative importance of these factors varies over space and time, as has been demonstrated in this study.

3.5.2. Trends for 1997–2007. We have considered trends in phytoplankton biomass, various climate indices and hydrodynamic variables, over the period 1997–2007. Trends in hydrodynamic variables over the study period are much larger and often of opposite sign to those previously calculated (Johnston and Gabric, 2010) for 1958–2005 and this is illustrated in Figs. 9 and 10, which show stable long term trends in SST and SSS, respectively, as well as what appear to be recent changes in the trends.

Differences in SST trends, depending on the region and latitudinal zone, have been reported previously (Trenberth et al., 2007). Such differences have also been found in a recent study (Roemmich and Gilson, 2009), which compared mean Argo float data (2004–2007) with data from the World Ocean Atlas, 2001 (Boyer et al., 2002). The study found that, in the present study region south of Australia, SST was increasing between about 50 and 60°S and decreasing between about 40 and 50°S (no results were given south of 60°S). This is consistent with the plots from Fig. 9, including the magnitude of the trends. In addition, the present study also finds possible recent decreases in SST in 60–65°S (spring) and 65–70°S.

The recent trends in SSS (Fig. 10) are also consistent with those found in the study by Roemmich and Gilson (2009) and a similar one by Hosoda et al. (2009); that is, recent increases in SSS between 40 and 50°S and decreases south of there. These trends are also consistent with decreased precipitation in the northern zones (Bindoff et al., 2010; Helm et al., 2010) and increased precipitation, sea-ice and glacial melt near the Antarctic continent (Jacobs, 2006).

4. Conclusions

Using a combination of satellite, model and model reanalysis data, we have investigated the effect of interannual climate variability on phytoplankton biomass and primary productivity in the Australian sector of the Southern Ocean during the period 1997–2007. In 5° latitudinal zones that approximate the frontal zones of the ACC, factors that affect chlorophyll-*a* and primary productivity have been identified and examined and have been found to be very similar.

Apart from sea-ice concentration, which is negatively correlated with both chlorophyll-*a* and primary productivity near the Antarctic continent, very different factors are found to influence both chlorophyll-*a* and primary productivity in spring compared with summer. In spring, the important factors are PAR, SST, MLD and stratification, bearing in mind that some of these factors covary. In the north in the 40–45°S zone, PDO and stratification are positively correlated with chlorophyll-*a* in summer, in contrast to zones further south. In summer in the zones near to and just north of the Polar Front (50–60°S), PAR and SST are the most important factors, with SST negatively correlated with chlorophyll-*a*. We find a number of covarying factors that influence chlorophyll-*a* in the zone (60–65°S) south of the Polar Front, where entrainment of UCDW brings nutrient-rich water to the near-surface. However, a multiple linear regression finds that 55% of the variance in chlorophyll-*a* in summer can be explained by a combination of SST (negative correlation) and mean wind stress (positive), whereas, in the 65–70°S zone in summer, sea-ice concentration (negative correlation) and SAM (positive) explain 51% of the variance in chlorophyll-*a*.

Over the period 1997–2007, we find that chlorophyll-*a* is decreasing in 55–60°S in both spring and summer, while both chlorophyll-*a* and primary productivity are increasing in 40–50°S in summer. A decrease in the Ekman transport of nutrients (iron) and an increase in SST, which is negatively correlated with chlorophyll-*a*, is consistent with the negative trend in chlorophyll-*a* found in summer in the 55–60°S zone. However, the similar trend in chlorophyll-*a* found in spring may be related to trends in Ekman transport and stratification rather than SST. The trends in the 40–50°S zone do not appear to be related to trends in the hydrological variables studied here.

Many of the trends for the hydrodynamic variables for 1997–2007 are of opposite sign and up to an order of magnitude larger those found previously (Johnston and Gabric, 2010) for the 1958–2005 time period. For example, an increasingly positive trend in SST is found in 50–60°S in recent years, consistent with a recent study using Argo float data (Roemmich and Gilson, 2009). Trends in sea-surface salinity are of opposite sign depending on which latitudinal zone is considered—south of the PF salinity is decreasing and north of the PF it is increasing,

again consistent with recent Argo float studies (Roemmich and Gilson, 2009; Hosoda et al., 2009) and precipitation studies (Bindoff et al., 2010; Helm et al., 2010). An investigation into these and other similar trends finds a discernible change in recent years in many cases, which is outside the bounds of earlier variability. This may indicate that there has been a shift in the last 10–15 yr in the ocean state of the Southern Ocean.

5. Acknowledgments

Support from Australian Antarctic Division grant, AAS Project 2784 and the Australian Research Network for Earth System Science (ARCNESS) is gratefully acknowledged. The authors would like to thank Benjamin Giese for providing SODA 5-d data sets. Some data used in this paper were produced with the Giovanni on-line data system, developed and maintained by the NASA GES DISC. We acknowledge the mission scientists and associated NASA personnel for the productivity of the SeaWiFS data. The authors also wish to acknowledge the use of the Ferret program (a product of NOAA's Pacific Marine Environmental Laboratory) for analysis and graphics in this study. MEI data was obtained from http://www.esrl.noaa.gov/psd/people/klaus.wolter/MEI/table.htm, SODA data was obtained from http://dsrs.atmos.umd.edu/DATA, SAM data fromwww.nerc-bas.ac.uk/icd/gjma/sam.html, PDO data from http://jisao.washington.edu/pdo/PDO.latest, VGPM data from http://www.science.oregonstate.edu/ocean.productivity/, sea-ice concentration data from http://nsidc.org/data/docs/daac/nsidc0079_bootstrap_seaice.gd.html and chlorophyll-*a* and PAR data from http://oceancolor.gsfc.nasa.gov/cgi/l3.

References

Aoki, S., Yoritaka, M. and Masuyama, A. 2003. Mulidecadal warming of subsurface temperature in the Indian sector of the Southern Ocean. *J. Geophys. Res.* **108**(C4), 8081, doi:10.1029/2000JC000307.

Arrigo, K. R., van Dijken, G. L. and Bushinsky, S. 2008. Primary production in the Southern Ocean, 1997-2006. *J. Geophys. Res.* **113**, C08004, doi:10.1029/2007JC004551.

Barbini, R., Colao, F., Fantoni, R., Fiorani, L., Okladnikova, I. G., and co-authors. 2005. LIDAR calibrated satellite sensed primary production in the Southern Ocean. *J. Optoelectron. Adv. M.* **7**(2), 1091–1101.

Behrenfeld, M. J. and Falkowski, P. G. 1997. Photosynthetic rates derived from satellite-based chlorophyll concentration. *Limnol. Oceanogr.* **42**, 1–20.

Behrenfeld, M. J., O'Malley, R. T., Siegel, D. A., McClain, C. R., Sarmiento, J. L., and co-authors. 2006. Climate-driven trends in contemporary ocean productivity. *Nature* **444**(7120), 752–755.

Behrenfeld, M. J., Siegel, D. A., O'Malley, R. T. and Maritorena, S. 2009. Global ocean phytoplankton. *Special Suppl. to Bull. Amer. Meteorol. Soc.* **90**(8), S68–S73.

Bindoff, N. L., Helm, K. P., Meijers, A. and Downes, S. 2010. The evolving state of Antarctica and Southern Ocean over the last three decades, *Atmosphere, Ocean, Environment and Society*, Vol. Conference Abstracts, AMOS, p. 9.

Böning, C. W., Dispert, A., Visbeck, M., Rintoul, S. R. and Schwarzkopf, F. U. 2008. The response of the Antarctic Circumpolar Current to recent climate change. *Nat. Geosci.* **1**(12), 864–869.

Boyce, D. G., Lewis, M. R. and Worm, B. 2010. Global phytoplankton decline over the past century. *Nature* **466**(7306), 591–596.

Boyer, T. P., Levitus, S., Antonov, J. I., Locarnini, R. and Garcia, H. E. 2005. Linear trends in salinity for the World Ocean, 1955-1998. *Geophys. Res. Lett.* **32**, L01604, doi:10.1029/2004GL021791.

Boyer, T., Stephens, C., Antonov, J., Corkwright, M. E., Locarnini, R. A., and co-authors. 2002. World Ocean Atlas 2001 (ed. Levitus, S.) Vol. 2, Salinity, NOAA Atlas NESDIS 50 U.S. Government Printing Office, Washington, DC.

Carr, M. E., Friedrichs, M. A. M., Schmeltz, M., Aita, M. N., Antoine, D. and co-authors. 2006. A comparison of global estimates of marine primary production from ocean color. *Deep-Sea Res. Part II-Top. Stud. Oceanogr.* **53**(5-7), 741–770.

Carton, J. A., Chepurin, G., Cao, X. H. and Giese, B. 2000. A Simple Ocean Data Assimilation analysis of the global upper ocean 1950-95. Part I: methodology. *J. Phys. Oceanogr.* **30**(2), 294–309.

Carton, J. A. and Giese, B. S. 2008. A reanalysis of ocean climate using SODA. *Mon. Wea. Rev.* **136**(8), 2999–3017.

Comiso, J. 1999, updated 2008. Bootstrap sea ice concentrations from NIMBUS-7 and DMSP SSM/I, 1997-2007, National Snow and Ice Data Center, Boulder, Colorado, USA.

Constable, A. J., Nicol, S. and Strutton, P. G. 2003. Southern Ocean productivity in relation to spatial and temporal variation in the physical environment. *J. Geophys. Res.* **108**(C4), 8079, doi:10.1029/2001JC001270.

de Baar, H. J. W., Boyd, P. W., Coale, K. H., Landry, M. R., Tsuda, A. and co-authors. 2005. Synthesis of iron fertilization experiments: from the iron age in the age of enlightenment. *J. Geophys. Res.* **110**, C09S16, doi:10.1029/2004JC002601.

Dierssen, H. M., Vernet, M. and Smith, R. C. 2000. Optimising models for remotely estimating primary production in Antarctic coastal waters. *Antarct. Sci.* **12**, 20–32.

Gabric, A. J., Cropp, R. A., McTainsh, G. H., Johnston, B. M., Butler, H. and co-authors. 2010. Australian dust storms in 2002-2003 and their impact on Southern Ocean biogeochemistry. *Glob. Biogeochem. Cycle* **24**, GB2005, doi:10.1029/2009GB003541.

Gilbert, R. O. 1987. *Statistical methods for environmental pollution monitoring.* Van Nostrand Reinhold Company Inc., New York.

Gille, S. T. 2002. Warming of the Southern Ocean since the 1950s. *Science* **295**(5558), 1275–1277.

Gille, S. T. 2008. Decadal-scale temperature trends in the Southern Hemisphere Ocean. *J. Clim.* **21**(18), 4749–4765.

Helm, K. P., Bindoff, N. L. and Church, J. A. 2010. Changes in the global hydrological-cycle inferred from ocean salinity. *Geophys. Res. Lett.* **37**, L18701, doi:10.1029/2010GL044222.

Henson, S. A., Sarmiento, J. L., Dunne, J. P., Bopp, L., Lima, I. and co-authors. 2010. Detection of anthropogenic climate change in satellite records of ocean chlorophyll and productivity. *Biogeosciences* **7**(2), 621–640.

Hess, A., Iyer, H. and Malm, W. 2001. Linear trend analysis: a comparison of methods. *Atmos. Environ.* **35**(30), 5211–5222.

Hill, K. L., Rintoul, S. R., Coleman, R. and Ridgway, K. R. 2008. Wind forced low frequency variability of the East Australia Current. *Geophys. Res. Lett.* **35**, L08602, doi:10.1029/2007GL032912.

Hirsch, R. M., Slack, J. R. and Smith, R. A. 1982. Techniques of trend analysis for monthly water quality data. *Water Resour. Res.* **18**, 107–121.

Hoppema, M., de Baar, H. J. W., Fahrbach, E., Hellmer, H. H. and Klein, B. 2003. Substantial advective iron loss diminishes phytoplankton production in the Antarctic Zone. *Glob. Biogeochem. Cycle* **17**(1), 1025, doi:10.1029/2002GB001957.

Hosoda, S., Suga, T., Shikama, N. and Mizuno, K. 2009. Global surface layer salinity change detected by Argo and its implication for hydrological cycle intensification. *J. Oceanogr.* **65**(4), 579–586.

Jacobs, S. 2006. Observations of change in the Southern Ocean. *Philos. Trans. R. Soc. A-Math. Phys. Eng. Sci.* **364**(1844), 1657–1681.

Johnston, B. M. and Gabric, A. J. 2010. Long-term trends in upper ocean structure and meridional circulation in the Southern Ocean south of Australia derived from the SODA reanalysis. *Tellus* **62A**, 719–736.

Large, W. G., McWilliams, J. C. and Doney, S. C. 1994. Oceanic vertical mixing—a review and a model with a nonlocal boundary-layer parameterization. *Rev. Geophys.* **32**(4), 363–403.

Le Quere, C., Rödenbeck, C., Buitenhuis, E. T., Conway, T. J., Langenfelds, R. and co-authors. 2007. Saturation of the Southern Ocean CO_2 sink due to recent climate change. *Science* **316**(5832), 1735–1738.

Levitus, S., Antonov, J. and Boyer, T. 2005. Warming of the world ocean, 1955-2003. *Geophys. Res. Lett.* **32**, L02604, doi:10.1029/2004GL021592.

Lovenduski, N. S. and Gruber, N. 2005. Impact of the Southern Annular Mode on Southern Ocean circulation and biology. *Geophys. Res. Lett.* **32**, L11603, doi:10.1029/2005GL022727.

Lovenduski, N. S., Gruber, N., Doney, S. C. and Lima, I. D. 2007. Enhanced CO2 outgassing in the Southern Ocean from a positive phase of the Southern Annular Mode. *Glob. Biogeochem. Cycle* **21**, GB2026, doi:10.1029/2006GB002900.

Mantua, N. J. and Hare, S. R. 2002. The Pacific decadal oscillation. *J. Oceanogr.* **58**(1), 35–44.

Marshall, G. J. 2003. Trends in the Southern Annular Mode from observations and reanalyses. *J. Clim.* **16**(24), 4134–4143.

Martin, J. H., Gordon, R. M. and Fitzwater, S. E. 1990. Iron in Antarctic waters. *Nature* **345**(6271), 156–158.

Martinez, E., Antoine, D., D'Ortenzio, F. and Gentili, B. 2009. Climate-driven basin-scale decadal oscillations of oceanic phytoplankton. *Science* **326**(5957), 1253–1256.

McClain, C. R., Feldman, G. C. and Hooker, S. B. 2004. An overview of the SeaWiFS project and strategies for producing a climate research quality global ocean bio-optical time series. *Deep-Sea Res. Part II-Top. Stud. Oceanogr.* **51**(1-3), 5–42.

Metzl, N. 2009. Decadal increase of oceanic carbon dioxide in Southern Indian Ocean surface waters (1991-2007). *Deep-Sea Res. Part II-Top. Stud. Oceanogr.* **56**(8-10), 607–619.

Mitchell, B. G. and Holm-Hansen, O. 1991. Observations and modeling of the Antarctic phytoplankton crop in relation to mixing depth. *Deep-Sea Res. Part A-Oceanogr. Res. Pap.* **38**(8-9), 981–1007.

Monaghan, A. J., Bromwich, D. H., Chapman, W. and Comiso, J. C. 2008. Recent variability and trends of Antarctic near-surface temperature. *J. Geophys. Res.* **113**, D04105, doi:10.1029/2007JD009094.

Montegut, C. D., Madec, G., Fischer, A. S., Lazar, A. and Iudicone, D. 2004. Mixed layer depth over the global ocean: An examination of profile data and a profile-based climatology. *J. Geophys. Res.* **109**, C12003, doi:10.1029/2004JC002378.

Monterey, G. and Levitus, S. 1997. U.S. Government Printing Office, chapter Seasonal Variability of Mixed Layer Depth for the World Ocean, p. 96.

Moore, J. K. and Doney, S. C. 2006. Remote sensing observations of ocean physical and biological properties in the region of the Southern Ocean Iron Experiment (SOFeX). *J. Geophys. Res.* **111**, C06026, doi:10.1029/2005JC003289.

Morel, A. and Berthon, J.-F. 1989. Surface pigments, algal biomass profiles, and potential production of the euphotic layer: Relationships reinvestigated in view of remote-sensing applications. *Limnol. Oceanogr.* **34**(8), 1545–1562.

Nicol, S., Pauly, T., Bindoff, N. L. and Strutton, P. G. 2000. 'BROKE' a biological/oceanographic survey off the coast of East Antarctica (80-150 degrees E) carried out in January-March 1996. *Deep-Sea Res. Part II-Top. Stud. Oceanogr.* **47**(12-13), 2281–2298.

Orsi, A. H., Whitworth, T. and Nowlin, W. D. 1995. On the meridional extent and fronts of the Antarctic Circumpolar Current. *Deep-Sea Res. Part I-Oceanogr. Res. Pap.* **42**(5), 641–673.

Orsi, A. and Ryan, U. 2001, updated 2006. Locations of the various fronts in the southern ocean, Australian Antarctic Data Centre - CAASM Metadata (http://data.aad.gov.au/aadc/metadata/).

Roemmich, D. and Gilson, J. 2009. The 2004-2008 mean and annual cycle of temperature, salinity, and steric height in the global ocean from the Argo Program. *Prog. Oceanogr.* **82**(2), 81–100.

Rose, J. M., Feng, Y., DiTullio, G. R., Dunbar, R. B., Hare, C. E. and co-authors. 2009. Synergistic effects of iron and temperature on Antarctic phytoplankton and microzooplankton assemblages. *Biogeosciences* **6**(12), 3131–3147.

Saba, V. S., Friedrichs, M. A. M., Antoine, D., Armstrong, R. A., Asanuma, I. and co-authors. 2010a. An evaluation of ocean color model estimates of marine primary productivity in coastal and pelagic regions across the globe. *Biogeosciences Discuss.* **7**(5), 6749–6788.

Saba, V. S., Friedrichs, M. A. M., Carr, M.-E., Antoine, D., Armstrong, R. A. and co-authors. 2010b. Challenges of modeling depth-integrated marine primary productivity over multiple decades: A case study at BATS and HOT. *Global Biogeochem. Cycles* **24**, GB3020, doi:10.1029/2009GB003655.

Schott, F. A., Stramma, L., Giese, B. S. and Zantopp, R. 2009. Labrador Sea convection and subpolar North Atlantic Deep Water export in the SODA assimilation model. *Deep-Sea Res. Part I-Oceanogr. Res. Pap.* **56**(6), 926–938.

Schott, F. A., Stramma, L., Wang, W., Giese, B. S. and Zantopp, R. 2008. Pacific subtropical cell variability in the SODA 2.0.2/3 assimilation. *Geophys. Res. Lett.* **35**, L10607, doi:10.1029/2008GL033757.

Sedwick, P. N., Bowie, A. R. and Trull, T. W. 2008. Dissolved iron in the Australian sector of the Southern Ocean (CLIVAR SR3 section): Meridional and seasonal trends. *Deep-Sea Res. Part I-Oceanogr. Res. Pap.* **55**(8), 911–925.

Sievers, H. A. and Nowlin, W. D. 1984. The stratification and water masses at Drake Passage. *J. Geophys. Res.-Oceans* **89**(NC6), 489–514.

Smith, W. O. and Comiso, J. C. 2008. Influence of sea ice on primary production in the Southern Ocean: A satellite perspective. *J. Geophys. Res.* **113**, C05S93, doi:10.1029/2007JC004251.

Smith, W. O., Marra, J., Hiscock, M. R. and Barber, R. T. 2000. The seasonal cycle of phytoplankton biomass and primary productivity in the Ross Sea, Antarctica. *Deep-Sea Res. Part II-Top. Stud. Oceanogr.* **47**(15-16), 3119–3140.

Smith, W. O. and Nelson, D. M. 1985. Phytoplankton bloom produced by a receding ice edge in the Ross Sea - Spatial coherence with the density field. *Science* **227**(4683), 163–166.

Sokolov, S. 2008. Chlorophyll blooms in the Antarctic Zone south of Australia and New Zealand in reference to the Antarctic Circumpolar Current fronts and sea ice forcing. *J. Geophys. Res.* **113**, C03022, doi:10.1029/2007JC004329.

Sokolov, S. and Rintoul, S. R. 2002. Structure of Southern Ocean fronts at 140 degrees E. *J. Mar. Syst.* **37**(1-3), 151–184.

Spencer, M. W., Wu, C. L. and Long, D. G. 2000. Improved resolution backscatter measurements with the SeaWinds pencil-beam scatterometer. *IEEE Trans. Geosci. Remote Sens.* **38**, 89–104.

Steinacher, M., Joos, F., Frölicher, T. L., Bopp, L., Cadule, P. and co-authors. 2010. Projected 21st century decrease in marine productivity: a multi-model analysis. *Biogeosciences* **7**, 979–1005.

Takahashi, T., Sutherland, S. C., Wanninkhof, R., Sweeney, C., Feely, R. A. and co-authors. 2009. Climatological mean and decadal change in surface ocean pCO2, and net sea-air CO2 flux over the global oceans. *Deep-Sea Res. Part II-Top. Stud. Oceanogr.* **56**(8-10), 554–577.

Thompson, D. W. J. and Solomon, S. 2002. Interpretation of recent Southern Hemisphere climate change. *Science* **296**(5569), 895–899.

Trenberth, K., Jones, P., Ambenje, P., Bojariu, R., Easterling, D. and co-authors. 2007. Climate change 2007: The Physical Science basis. Contribution of working group I to the Fourth Assessment Report of the Intergovernmental Panel on Climate Change. In: *Observations: Surface and Atmospheric Climate Change*, (eds S. Solomon, D. Qin, M. Manning, Z. Chen, M. Marquis, K. Averyt, M. Tignor and H. Miller). Cambridge University Press, Cambridge.

Uppala, S., Kållberg, P., Simmons, A., Andrae, U., da CostaBechtold, V. and co-authors. 2005. The ERA-40 re-analysis. *Quart. J. Roy. Meteor. Soc.* **131**, 2961–3012.

Venables, H. and Moore, C. M. 2010. Phytoplankton and light limitation in the Southern Ocean: learning from high-nutrient, high-chlorophyll areas. *J. Geophys. Res.* **115**, C02015, doi:10.1029/2009JC005361.

Visbeck, M. 2009. A station based Southern Annular Mode index from 1884-2005. *J. Clim.* **22**(4), 940–950.

Whitehouse, M. J., Korb, R. E., Atkinson, A., Thorpe, S. E. and Gordon, M. 2008. Formation, transport and decay of an intense phytoplankton bloom within the High-Nutrient Low-Chlorophyll belt of the Southern Ocean. *J. Mar. Syst.* **70**, 150–167.

Wolter, K. 1987. The Southern Oscillation in surface circulation and climate over the tropical Atlantic, Eastern Pacific, and Indian Oceans as captured by cluster analysis. *J. Climate Appl. Meteor.* **26**(4), 540–558.

Wolter, K. and Timlin, M. S. 1993. Monitoring ENSO in COADS with a seasonally adjusted principal component index, *Proc. of the 17th Climate Diagnostics Workshop*, Oklahoma Clim. Survey, NOAA/N MC/CAC, CIMMS and the School of Meteor., Univ. of Oklahoma, pp. 52–57.

Yang, X.-Y., Dongxiao, D., Wang, J. and Huang, R. X. 2007. Connection between the decadal variabitity in the Southern Ocean circulation and the Southern Annular Mode. *Geophys. Res. Lett.* **34**, L16604, doi:10.1029/2007GL030526.

Zhang, J. 2007. Increasing Antarctic sea ice under warming atmospheric and oceanic conditions. *J. Clim.* **20**(11), 2515–2529.

Zheng, Y. and Giese, B. S. 2009. Ocean heat transport in Simple Ocean Data Assimilation: Structure and mechanisms. *J. Geophys. Res.* **114**, C11009, doi:10.1029/2008JC005190.